L-Shaped Tromino Rep-Tiles-Based Approach for the Design of Modular Planar Phased Arrays

N. Anselmi, L. Tosi, P. Rocca, and A. Massa

2024/03/18

Contents

1 Array 24×36

1.0.1 Parameters

- Number of elements: 24×36 elements array, grouped in 18 clusters of 48
- Number of rows: 24
- Number of columns: 36
- Samples: $u \rightarrow 702$, $v \rightarrow 462$
- Evaluated tilings: T =3412
- Elements spacing: $dx = dy = 0.5\lambda$

The cost function only considers the mask matching.

1.0.2 Results

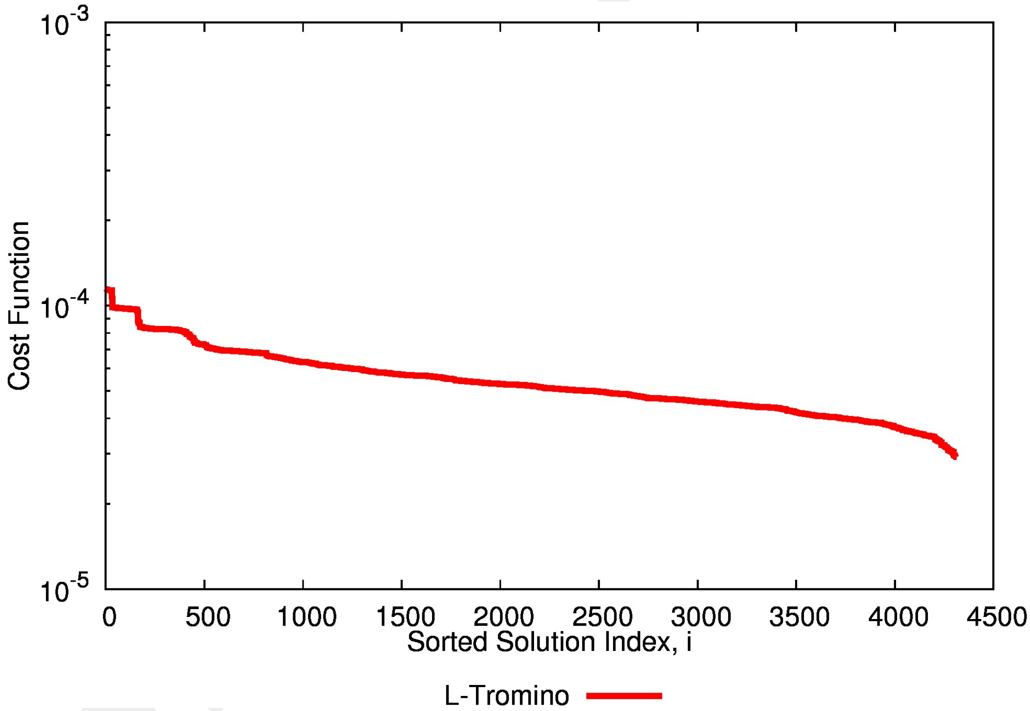

Figure 1: Solution index vs Cost function

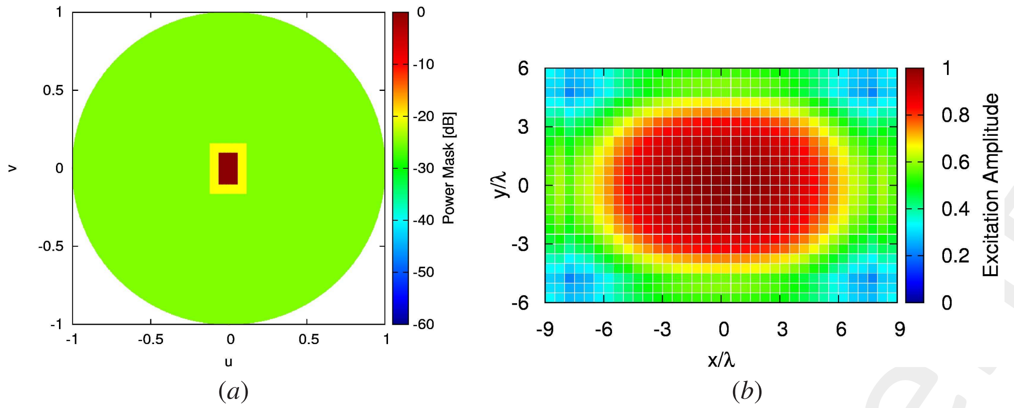

Figure 2: (*a*) Mask used for the computation of the cost function (*b*) Reference amplitudes

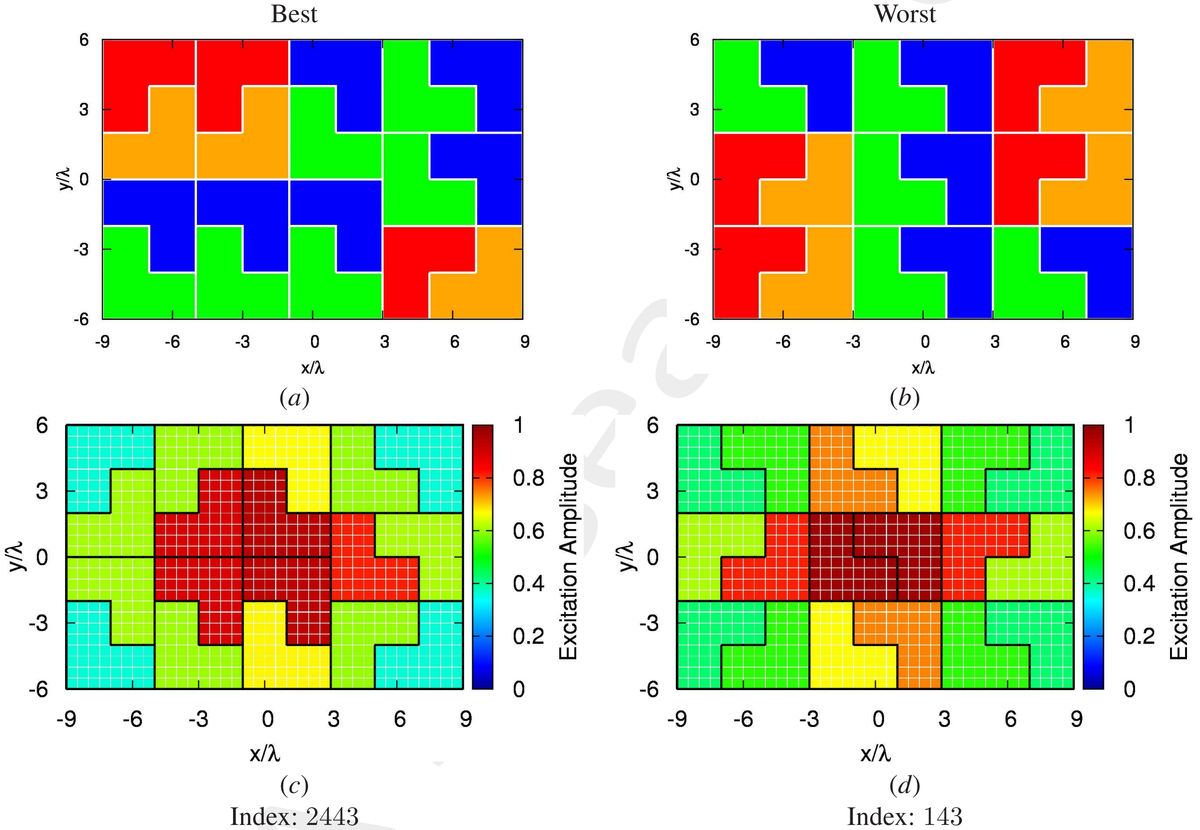

Figure 3: Numerical Assessment ($M = 6,\ N = 9$, $d = 0.5\lambda$, (θ_0,ϕ_0)=(0.0, 0.0) [deg]; $Q_I = 18$ for $I = 48$) - Plots of (*a*) optimal solution clustering and of the (*b*) worst solution clustering, with the respective (*c*) clustered excitations value for the best solution and (*d*) the clustered excitations for the worst performance solution.

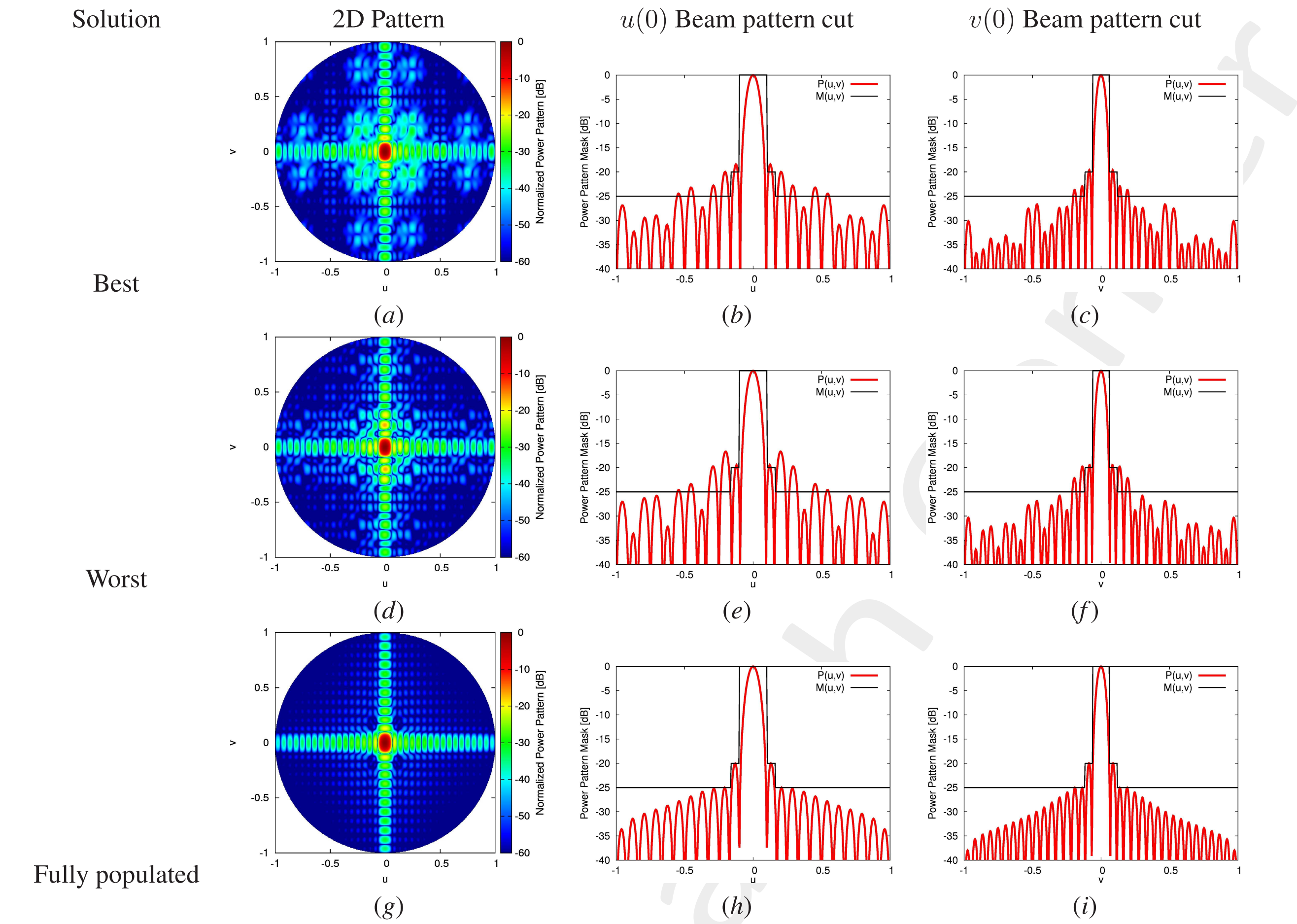

Figure 4: Numerical Assessment ($M = 6,\ N = 9,\ d = 0.5\lambda$, ($\theta_0$,$\phi_0$)=(0.0, 0.0) [deg]; $Q_I = 18$ for $I = 48$) - Plots of normalized power pattern radiated in the whole angular range ($-1 \leq u \leq 1,\ -1 \leq v \leq 1$) for (*a*) the best, (*d*) worst and (*g*) fully populated solution, along the $\phi = 0$ [deg] plane for best (*b*), worst (*e*) and fully populated (*h*) cases, and along the $\phi = 90$ [deg] plane for the best (*c*), worst (*f*) and fully populated (*i*) solution

Solution	SLL $[dB]$	Max. Directivity $[dBi]$	Mask Matching	HPBW (AZ) $[deg]$	HPBW (EL) $[deg]$
Best	-18.408	33.881	0.292×10^{-4}	3.14	4.57
Worst	-16.640	33.936	0.114×10^{-3}	3.07	4.50
Fully populated	-19.958	33.828	0.393×10^{-9}	3.17	4.77

Table I: Numerical Assessment ($M = 24,\ N = 36,\ d = 0.5\lambda$, ($\theta_0$,$\phi_0$)=(0.0, 0.0) [deg] - Pattern featuresObtained parameters

1.1 SLL -20 dB Symmetric Mask

L-Tromino, *Second Level Clustering* - Integral Difference Priority

For the second iteration it is possible to choose which tile of the "First Level" divide: the chosen criteria is to increase the number of tiles where the difference between the clustered amplitudes and the reference amplitudes was greater.

$$\xi_q = \frac{1}{\xi_{max}} \sum_{m=1}^{M} \sum_{n=1}^{N} |a_{mn} - a_q| \delta_{c_{mn}q} \tag{1}$$

The mask matching difference produced both by a reclustering of a single tile, Eq. 3 and by multiple tiles, Eq. 2 is then calculated to evaluate the impact of increasing the number of clusters with the upper level clustering method:

$$\Delta\Gamma_s^q = \Gamma_1 - \Gamma_2^q \tag{2}$$

$$\Delta_0\Gamma_c^{\{1,\ldots,q\}} = \Gamma_1 - \Gamma_2^{\{1,\ldots,q\}} \tag{3}$$

$$\Delta\Gamma_c^{\{1,\ldots,q\}} = \Gamma_2^{\{1,\ldots,q-1\}} - \Gamma_2^{\{1,\ldots,q\}} \tag{4}$$

ξ_q	q	$\Delta\Gamma_s^q$	$\%\Delta\Gamma_s^q$	$\Delta\Gamma_c^q$	$\%\Delta\Gamma_c^q$	$\Delta_0\Gamma_c^{\{1,\ldots,q\}}$	$\%\Delta_0\Gamma_c^{\{1,\ldots,q\}}$
1	18	0.568×10^{-5}	19.43	0.568×10^{-5}	19.43	0.568×10^{-5}	19.43
0.9285	9	0.522×10^{-5}	17.86	0.472×10^{-5}	16.13	0.104×10^{-4}	35.56
0.9033	10	0.383×10^{-5}	13.10	0.520×10^{-5}	9.25	0.131×10^{-4}	44.81
0.9033	16	0.397×10^{-5}	13.58	0.250×10^{-5}	8.55	0.156×10^{-4}	53.36
0.8337	8	0.438×10^{-5}	14.98	0.200×10^{-5}	6.84	0.176×10^{-4}	60.20
0.8337	5	0.426×10^{-5}	14.57	0.170×10^{-5}	5.82	0.193×10^{-4}	66.02
0.6825	15	0.140×10^{-5}	4.79	0.090×10^{-5}	3.08	0.202×10^{-4}	69.10
0.6053	6	0.845×10^{-7}	0.29	0.080×10^{-5}	2.74	0.210×10^{-4}	71.84
0.6053	7	0.666×10^{-7}	0.23	0.060×10^{-5}	2.05	0.216×10^{-4}	73.89
0.5962	1	0.237×10^{-5}	8.11	0.080×10^{-5}	2.73	0.224×10^{-4}	76.62
0.5962	2	0.267×10^{-5}	9.13	0.110×10^{-5}	3.08	0.233×10^{-4}	79.70
0.5962	3	0.226×10^{-5}	7.73	0.060×10^{-5}	2.06	0.239×10^{-4}	81.76
0.5962	4	0.222×10^{-5}	7.59	0.050×10^{-5}	1.71	0.244×10^{-4}	83.47
0.5623	17	-0.951×10^{-6}	-3.25	0.110×10^{-5}	3.76	0.255×10^{-4}	87.23
0.5289	12	-0.332×10^{-6}	-1.14	0.040×10^{-5}	1.37	0.259×10^{-4}	88.60
0.5289	14	-0.546×10^{-6}	-1.87	0.020×10^{-5}	0.68	0.261×10^{-4}	89.28
0.4976	11	0.66×10^{-6}	2.26	0.040×10^{-5}	1.37	0.265×10^{-4}	90.65
0.4813	13	-0.42×10^{-6}	-1.44	0.010×10^{-5}	0.34	0.266×10^{-4}	90.99

Table II: Re-Clustering priority and obtained Mask Matching

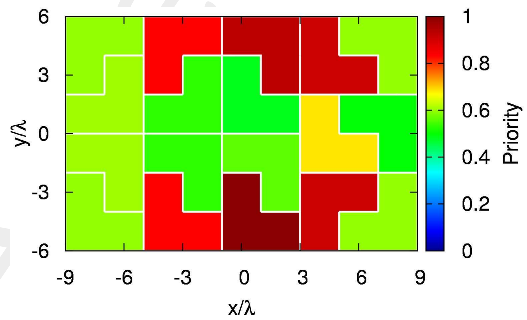

Figure 5: Integral difference priority for all tiles

The decision of the number of tiles to recluster can be taken looking at the graphs that represent the variation for each newly reclustered tile: when reclustering no longer improves the Γ parameter the reclustering process should be stopped.

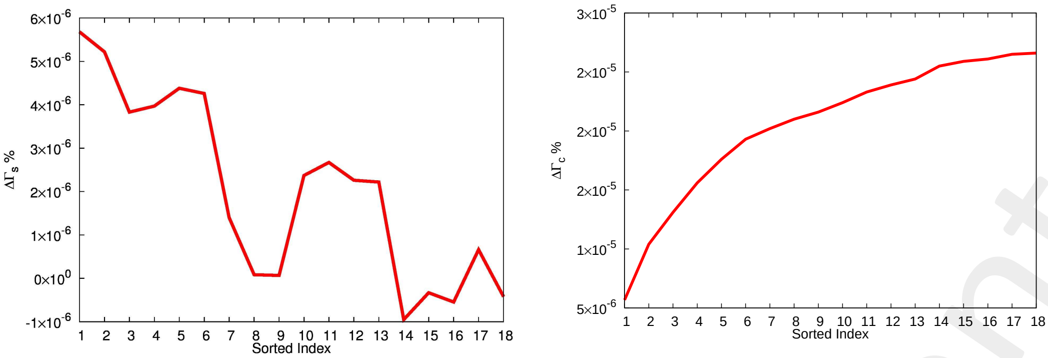

(a) (b)

Figure 6: Effect on Δ_Γ of the second level tiling (a) for the single second level clustered tile and (b) for the cumulative second level clustering of the tiles

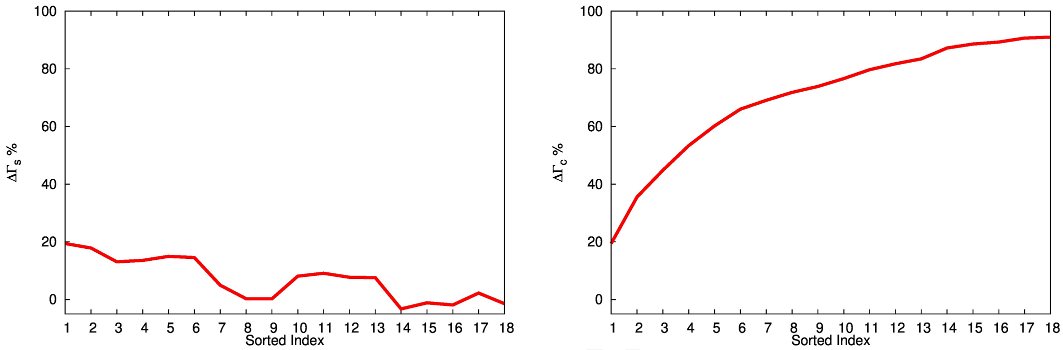

(a) (b)

Figure 7: Effect on $\%\Delta_\Gamma$ of the second level tiling (a) for the single second level clustered tile and (b) for the cumulative second level clustering of the tiles

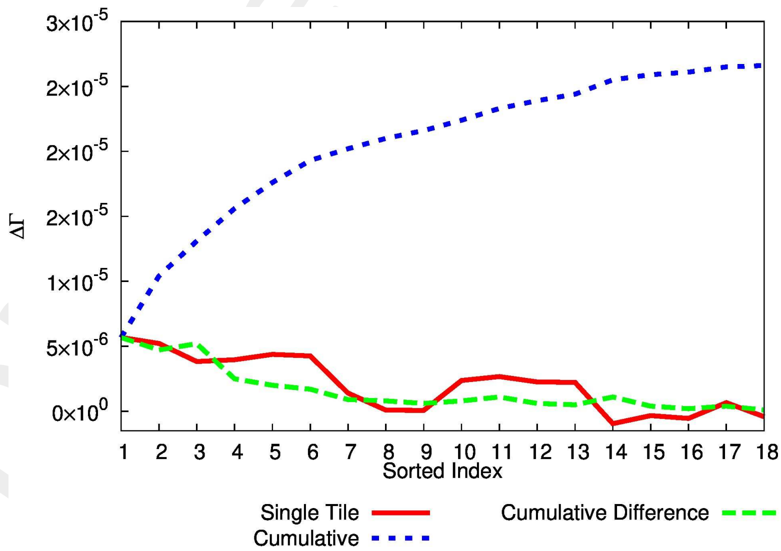

Figure 8: $\Delta\Gamma$ variations for single second level tile (red), for cumulative tiling with respect to the previous tile (green) and cumulative with respect to the first level tiling

A brief resume of the obtained results is shown to prove the effects of the cumulative reclustering:

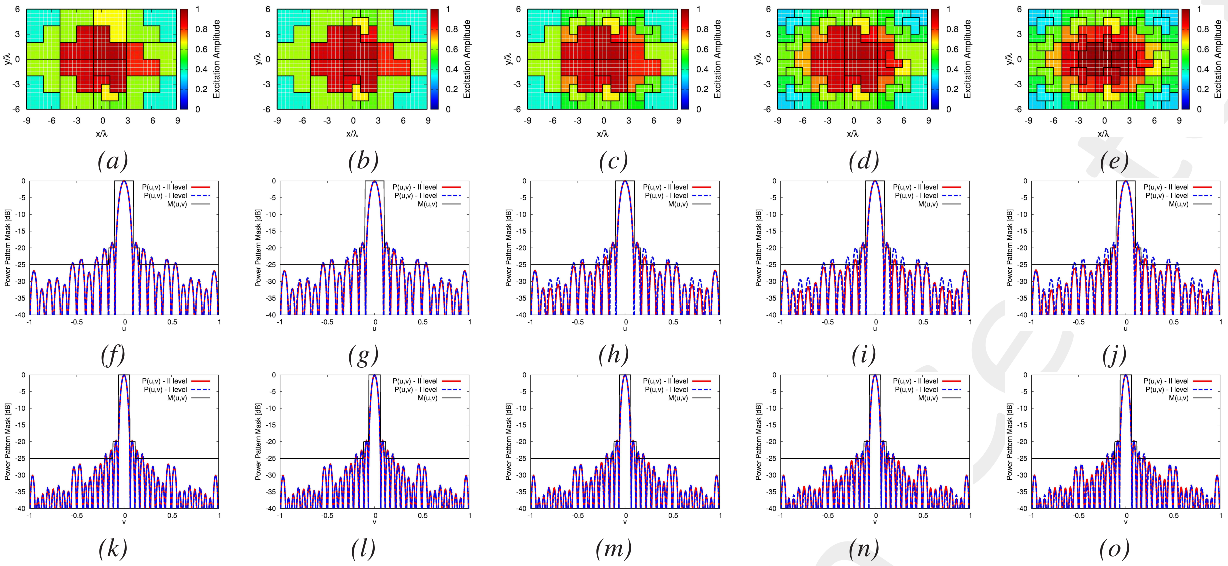

Figure 9: Numerical Assessment ($M = 24,\ N = 36$, $d = 0.5\lambda$, (θ_0,ϕ_0)=(0.0, 0.0) [deg]) - Plots of: (a) clustered amplitudes, power pattern along (f) the $\phi = 0$ [deg] plane and (k) $\phi = 90$ [deg] plane for **one** cluster tiled with II level subclusters; (b) clustered amplitudes, power pattern along (g) the $\phi = 0$ [deg] plane and (l) $\phi = 90$ [deg] plane for **two** clusters tiled with II level subclusters; (c) clustered amplitudes, power pattern along (h) the $\phi = 0$ [deg] plane and (m) $\phi = 90$ [deg] plane for **six** clusters tiled with II level subclusters; (d) clustered amplitudes, power pattern along (i) the $\phi = 0$ [deg] plane and (n) $\phi = 90$ [deg] plane for **twelve** clusters tiled with II level subclusters; (e) clustered amplitudes, power pattern along (j) the $\phi = 0$ [deg] plane and (o) $\phi = 90$ [deg] plane for **all** clusters tiled with II level subclusters;

I level	II level - 1 tile	II level - 2 tiles	II level - 6 tiles	II level - 12 tiles	II level - All tiles
0.292×10^{-4}	0.236×10^{-4}	0.189×10^{-4}	0.998×10^{-5}	0.529×10^{-5}	0.267×10^{-5}

Table III: Numerical Assessment ($M = 24,\ N = 36$, $d = 0.5\lambda$, (θ_0,ϕ_0)=(0.0, 0.0) [deg]) - Comparison of the obtained Mask Matching (Γ) obtained for the test cases

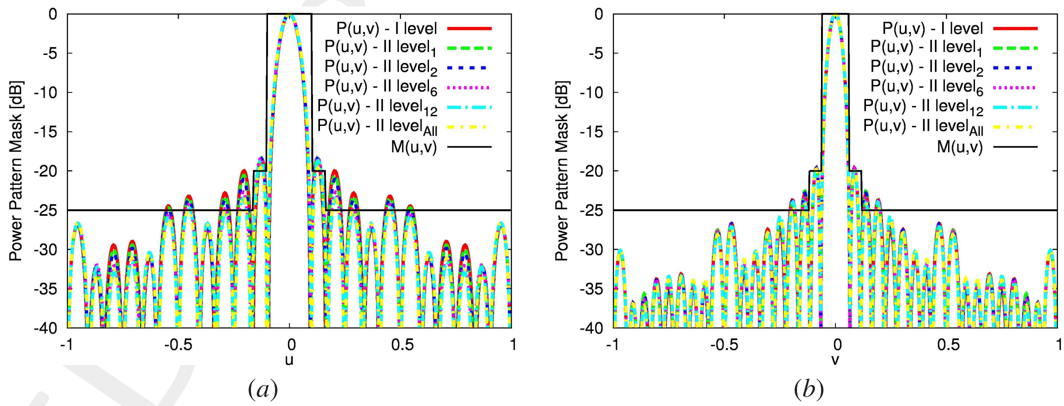

Figure 10: Numerical Assessment ($M = 24,\ N = 36$, $d = 0.5\lambda$, (θ_0,ϕ_0)=(0.0, 0.0) [deg]) - Plots of: (a) power pattern along (a) the $\phi = 0$ [deg] plane and (b) $\phi = 90$ [deg] plane for all the test cases

Parameters - II level clustering on the highest priority tile:

- Number of elements: 24×36 elements array
- Number of rows: $M = 24$ Number of columns: $N = 36$
- Number of clusters: $\sigma_1 = 17$, $\sigma_2 = 4$
- Clusters elements: $\gamma_1 = 48$, $\gamma_2 = 12$
- Samples: $u \to 702$, $v \to 462$
- Elements spacing: $dx = dy = 0.5\lambda$

The cost function only considers the mask matching.

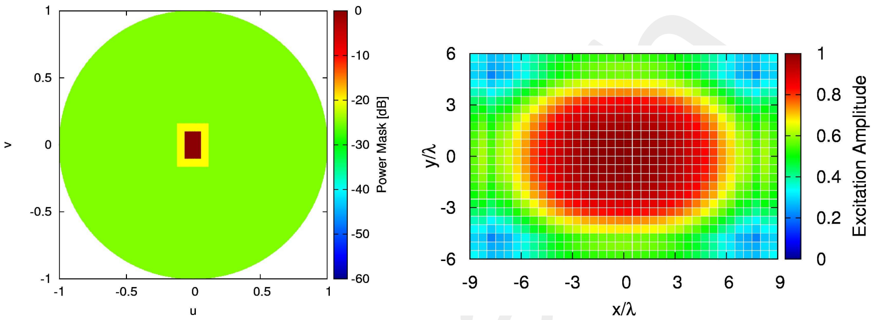

(*a*) (*b*)

Figure 11: (*a*) Mask used for the computation of the cost function (*b*) Reference amplitudes

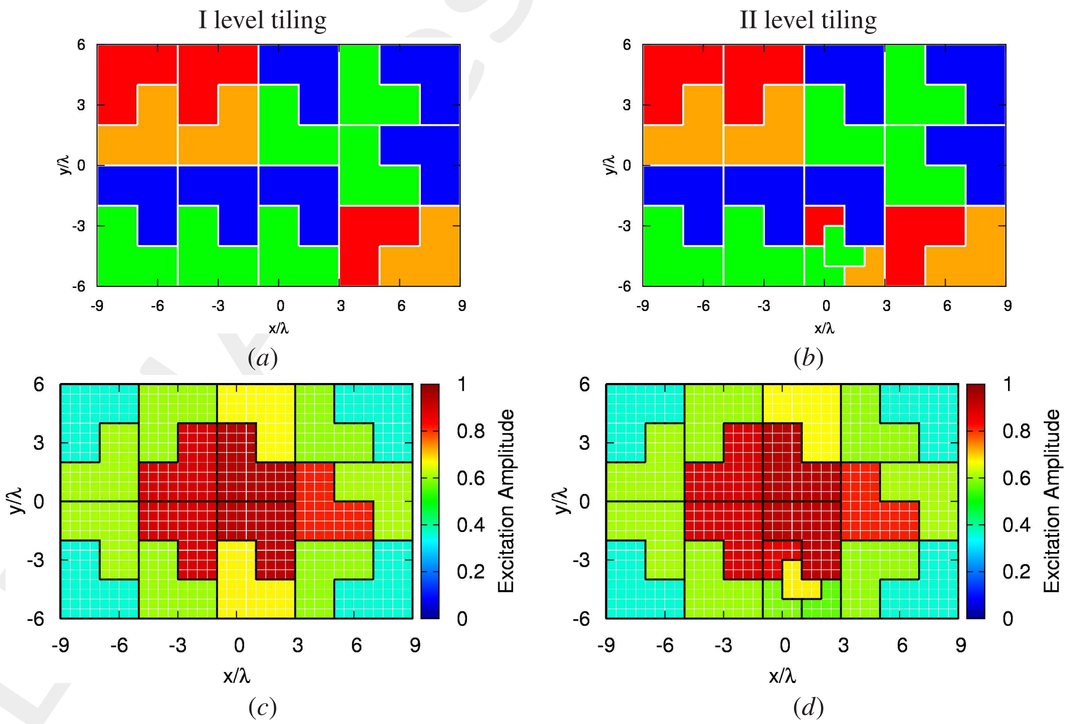

Figure 12: Numerical Assessment ($M = 24$, $N = 36$, $d = 0.5\lambda$, (θ_0,ϕ_0)=(0.0, 0.0) [deg]; $\sigma_1 = 17$ and $\sigma_1 = 4$ for $\gamma_1 = 48$ and $\gamma_2 = 12$) - Plots of (*a*) optimal solution clustering only with I level tiles and of the (*b*) same solution clustering with one cluster tiled with II level subclusters, with the respective (*c*) clustered excitations value for the I level solution and (*d*) the clustered excitations for the II level solution.

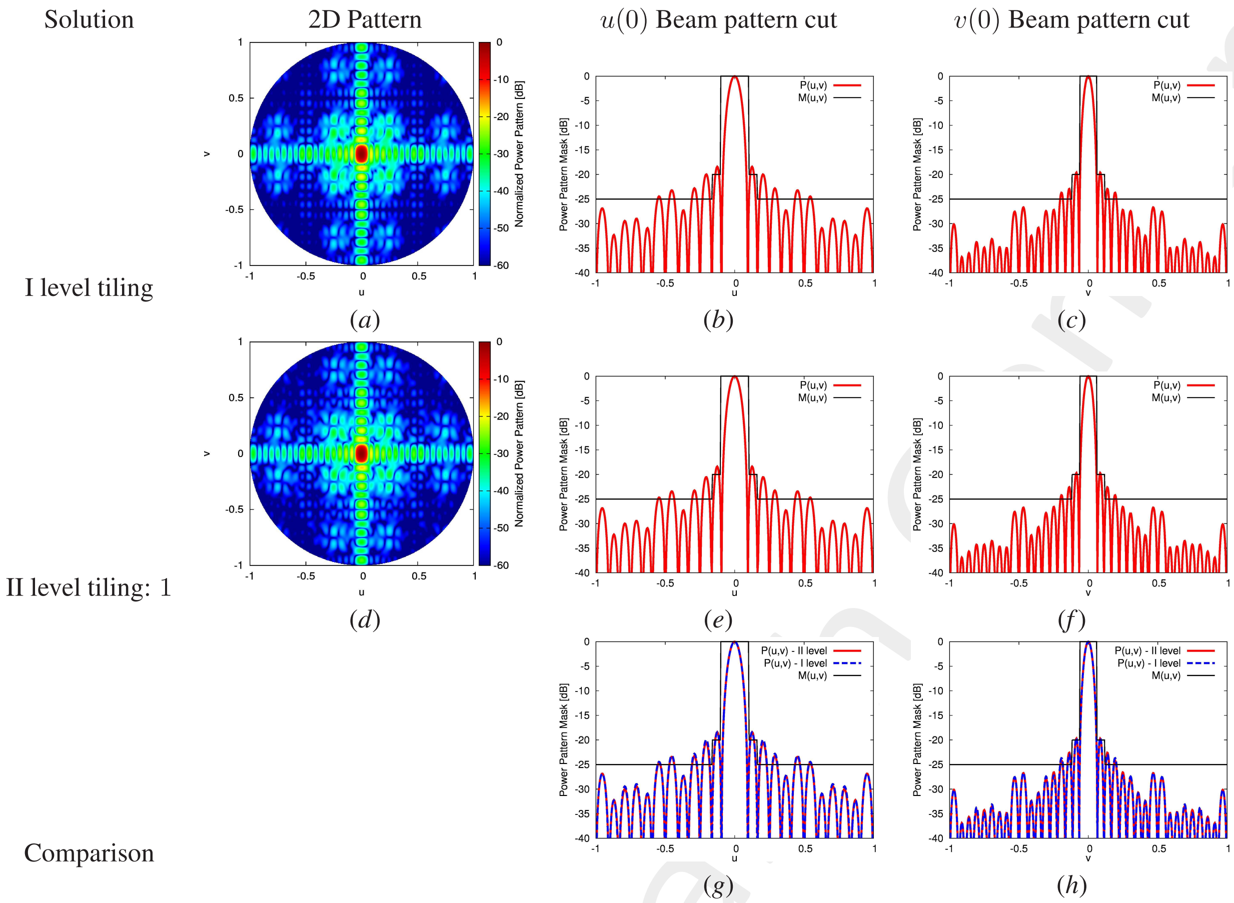

Figure 13: Numerical Assessment ($M = 24,\ N = 36$, $d = 0.5\lambda$, (θ_0,ϕ_0)=(0.0, 0.0) [deg]; $\sigma_1 = 17$ and $\sigma_2 = 4$ for $\gamma_1 = 48$ and $\gamma_2 = 24$) - Plots of normalized power pattern radiated in the whole angular range ($-1 \leq u \leq 1,\ -1 \leq v \leq 1$) for (*a*) the I level clustering, (*d*) II level clustering and, along the $\phi = 0$ [deg] plane for I level (*b*), II level (*e*) and the comparison between both (*g*) cases, and along the $\phi = 90$ [deg] plane for I level (*c*), II level (*f*) and comparison between both (*h*) solution

Solution	SLL $[dB]$	Max. Directivity $[dBi]$	Mask Matching	HPBW (AZ) $[deg]$	HPBW (EL) $[deg]$
I level	-18.408	33.881	0.292×10^{-4}	3.14	4.57
II level	-18.392	33.874	0.236×10^{-4}	3.14	4.59
Fully populated	-19.958	33.828	0.393×10^{-9}	3.17	4.77

Table IV: Numerical Assessment ($M = 24,\ N = 36$, $d = 0.5\lambda$, (θ_0,ϕ_0)=(0.0, 0.0) [deg] - Pattern features

Parameters - II level clustering on the two highest priority tiles:

- Number of elements: 24×36 elements array
- Number of rows: $M = 24$ Number of columns: $N = 36$
- Number of clusters: $\sigma_1 = 16$, $\sigma_2 = 8$
- Clusters elements: $\gamma_1 = 48$, $\gamma_2 = 12$
- Samples: $u \rightarrow 702$, $v \rightarrow 462$
- Elements spacing: $dx = dy = 0.5\lambda$

The cost function only considers the mask matching.

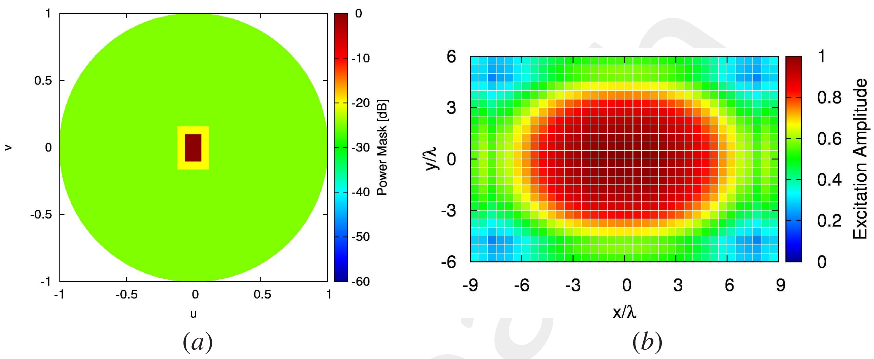

Figure 14: (a) Mask used for the computation of the cost function (b) Reference amplitudes

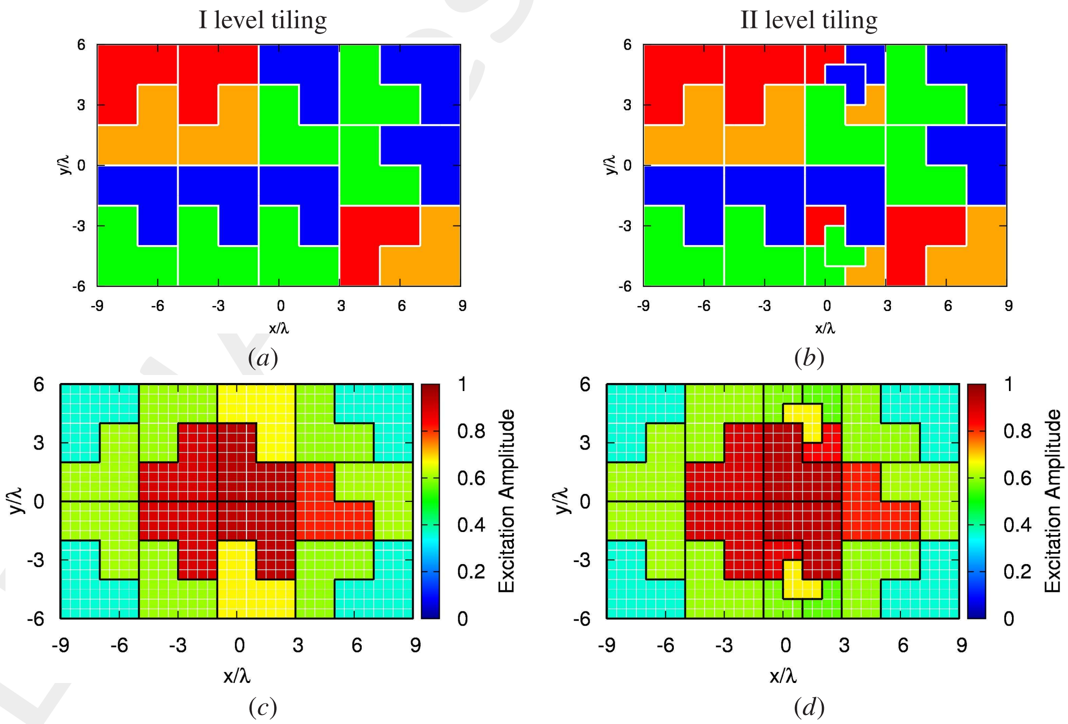

Figure 15: Numerical Assessment ($M = 24$, $N = 36$, $d = 0.5\lambda$, (θ_0,ϕ_0)=(0.0, 0.0) [deg]; $\sigma_1 = 16$ and $\sigma_2 = 8$ for $\gamma_1 = 48$ $\gamma_2 = 12$) - Plots of (a) optimal solution clustering only with I level tiles and of the (b) same solution clustering with two clusters tiled with II level subclusters, with the respective (c) clustered excitations value for the I level solution and (d) the clustered excitations for the II level solution.

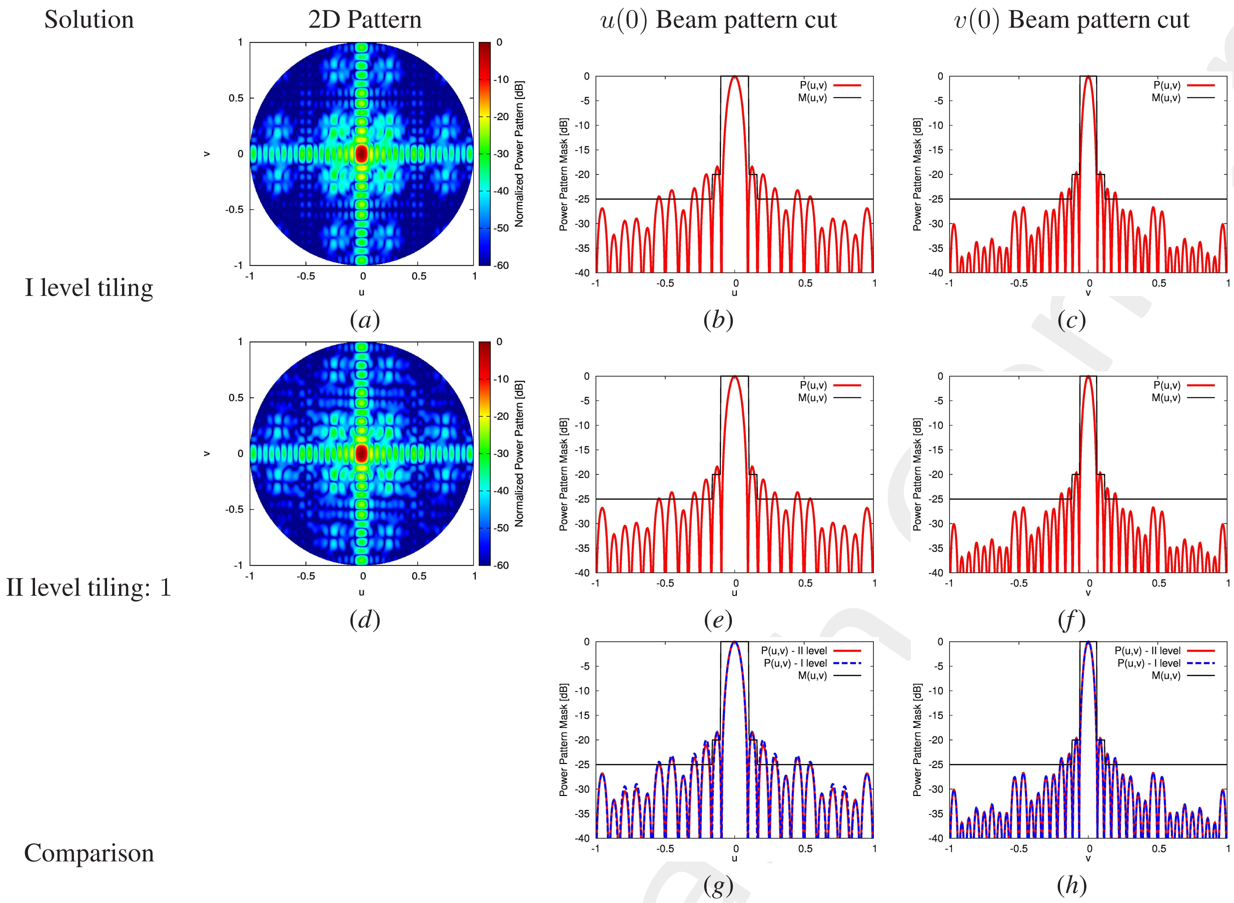

Figure 16: Numerical Assessment ($M = 24,\ N = 36$, $d = 0.5\lambda$, (θ_0,ϕ_0)=(0.0, 0.0) [deg]; $\sigma_1 = 16$ and $\sigma_2 = 8$ for $\gamma_1 = 48$ $\gamma_2 = 12$) - Plots of normalized power pattern radiated in the whole angular range ($-1 \leq u \leq 1,\ -1 \leq v \leq 1$) for ($a$) the I level clustering, (d) II level clustering and, along the $\phi = 0$ [deg] plane for I level (b), II level (e) and the comparison between both (g) cases, and along the $\phi = 90$ [deg] plane for I level (c), II level (f) and comparison between both (h) solution

Solution	SLL $[dB]$	Max. Directivity $[dBi]$	Mask Matching	HPBW (AZ) $[deg]$	HPBW (EL) $[deg]$
I level	-18.408	33.881	0.292×10^{-4}	3.14	4.57
II level	-18.391	33.868	0.189×10^{-4}	3.14	4.61
Fully populated	-19.958	33.828	0.393×10^{-9}	3.17	4.77

Table V: Numerical Assessment ($M = 24,\ N = 36$, $d = 0.5\lambda$, (θ_0,ϕ_0)=(0.0, 0.0) [deg] - Pattern features

Parameters - II level clustering on the six highest priority tiles:

- Number of elements: 24×36 elements array
- Number of rows: $M = 24$ Number of columns: $N = 36$
- Number of clusters: $\sigma_1 = 12$, $\sigma_2 = 24$
- Clusters elements: $\gamma_1 = 48$, $\gamma_2 = 12$
- Samples: $u \rightarrow 702$, $v \rightarrow 462$
- Elements spacing: $dx = dy = 0.5\lambda$

The cost function only considers the mask matching.

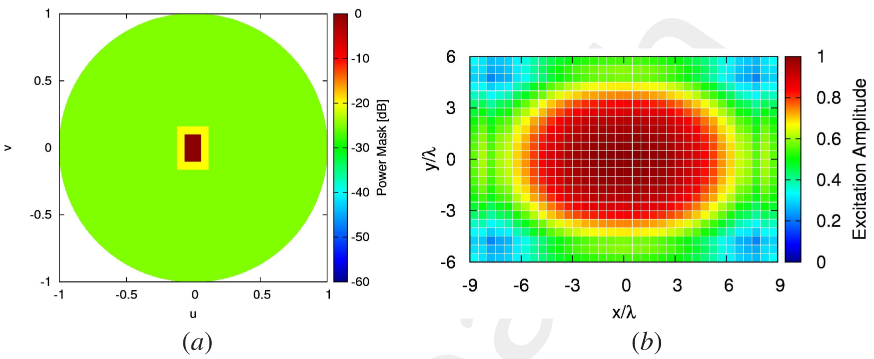

Figure 17: (a) Mask used for the computation of the cost function (b) Reference amplitudes

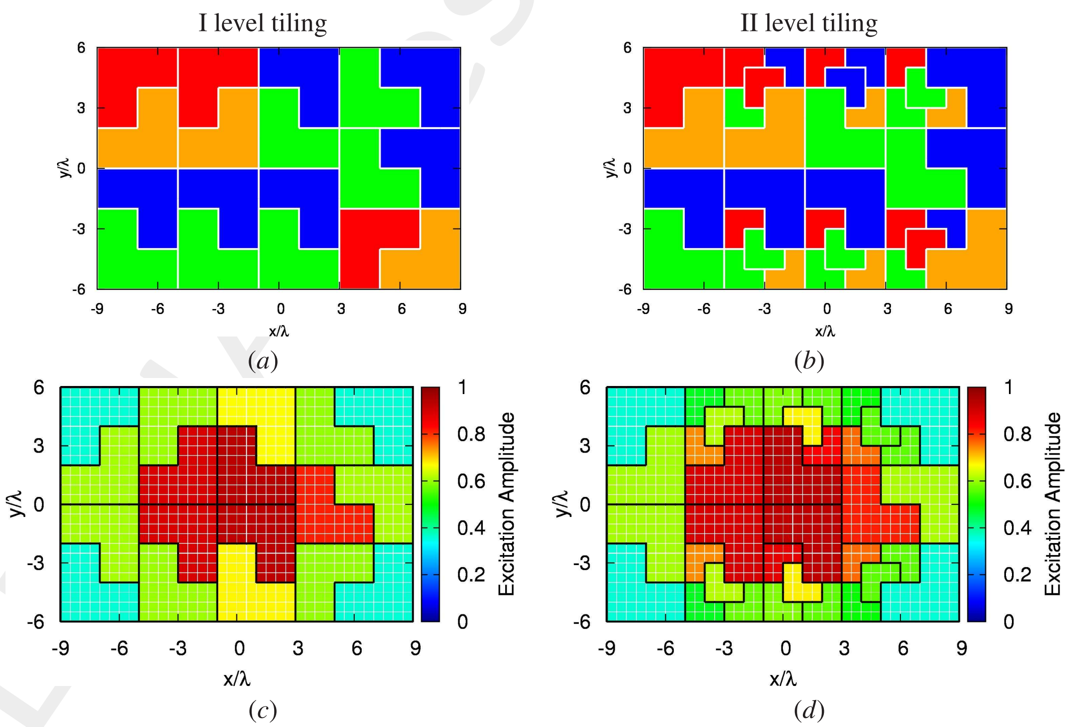

Figure 18: Numerical Assessment ($M = 24$, $N = 36$, $d = 0.5\lambda$, (θ_0,ϕ_0)=(0.0, 0.0) [deg]; $\sigma_1 = 12$ and $\sigma_2 = 24$ for $\gamma_1 = 48$ and $\gamma_2 = 12$) - Plots of (a) optimal solution clustering only with I level tiles and of the (b) same solution clustering with six clusters tiled with II level subclusters, with the respective (c) clustered excitations value for the I level solution and (d) the clustered excitations for the II level solution.

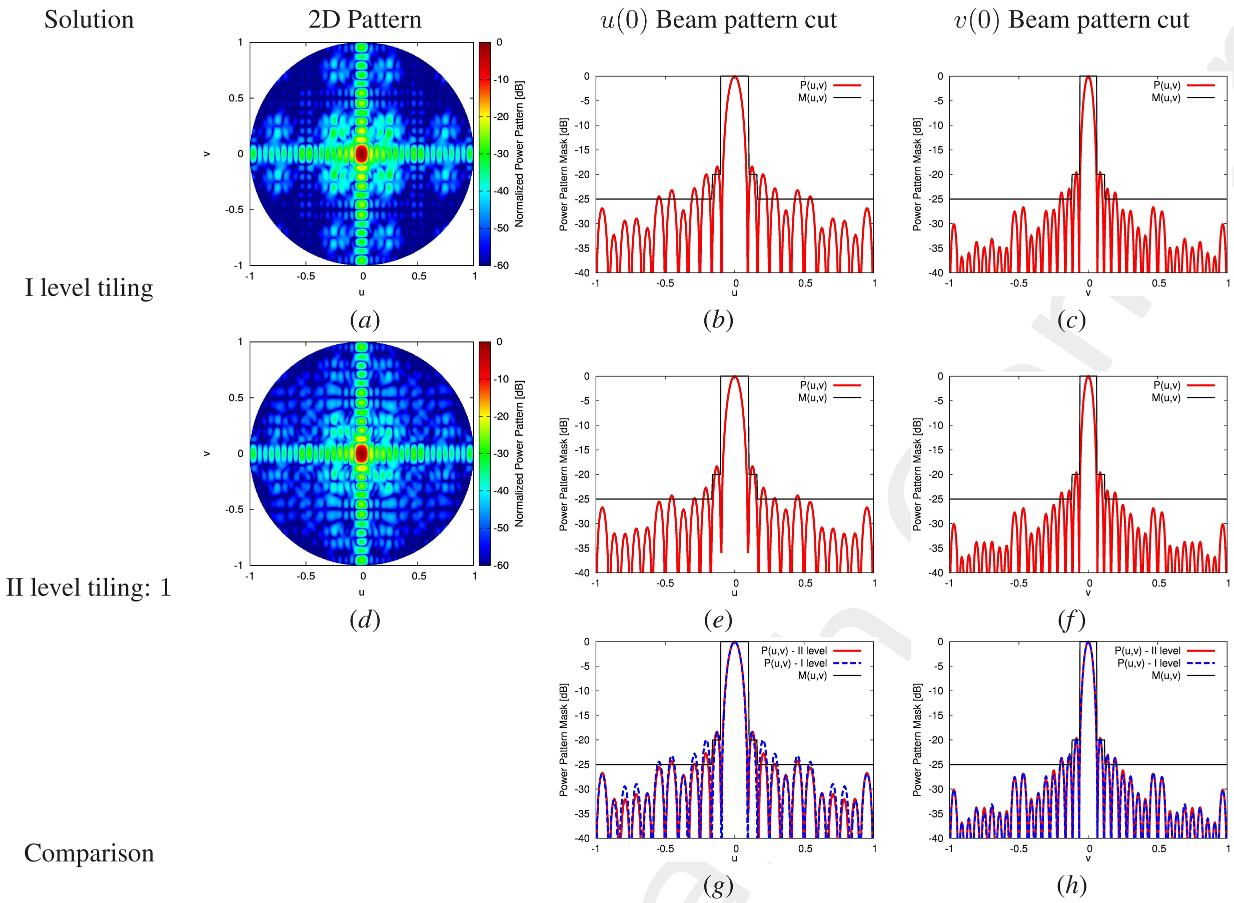

Figure 19: Numerical Assessment ($M = 24$, $N = 36$, $d = 0.5\lambda$, (θ_0,ϕ_0)=(0.0, 0.0) [deg]; $\sigma_1 = 12$ and $\sigma_2 = 24$ for $\gamma_1 = 48$ and $\gamma_2 = 12$) - Plots of normalized power pattern radiated in the whole angular range ($-1 \leq u \leq 1$, $-1 \leq v \leq 1$) for (a) the I level clustering, (d) II level clustering and, along the $\phi = 0$ [deg] plane for I level (b), II level (e) and the comparison between both (g) cases, and along the $\phi = 90$ [deg] plane for I level (c), II level (f) and comparison between both (h) solution

Solution	SLL $[dB]$	Max. Directivity $[dBi]$	Mask Matching	HPBW (AZ) $[deg]$	HPBW (EL) $[deg]$
I level	-18.408	33.881	0.292×10^{-4}	3.14	4.57
II level	-18.324	33.851	0.998×10^{-5}	3.14	4.66
Fully populated	-19.958	33.828	0.393×10^{-9}	3.17	4.77

Table VI: Numerical Assessment ($M = 24$, $N = 36$, $d = 0.5\lambda$, (θ_0,ϕ_0)=(0.0, 0.0) [deg] - Pattern features

Parameters - II level clustering on the twelve highest priority tiles:

- Number of elements: 24×36 elements array
- Number of rows: $M = 24$ Number of columns: $N = 36$
- Number of clusters: $\sigma_1 = 6$, $\sigma_2 = 48$
- Clusters elements: $\gamma_1 = 48$, $\gamma_2 = 12$
- Samples: $u \rightarrow 702$, $v \rightarrow 462$
- Elements spacing: $dx = dy = 0.5\lambda$

The cost function only considers the mask matching.

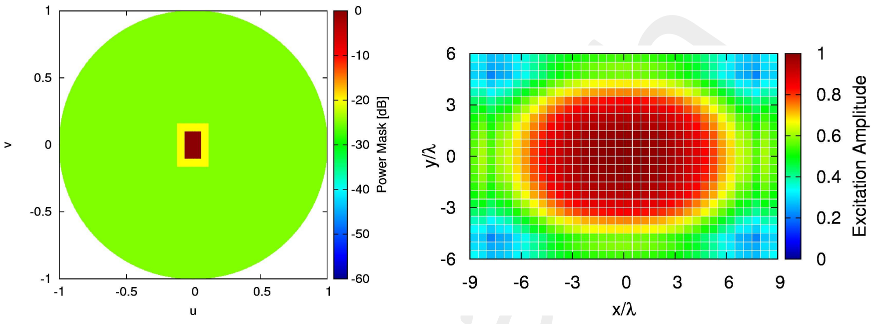

(a) (b)

Figure 20: (a) Mask used for the computation of the cost function (b) Reference amplitudes

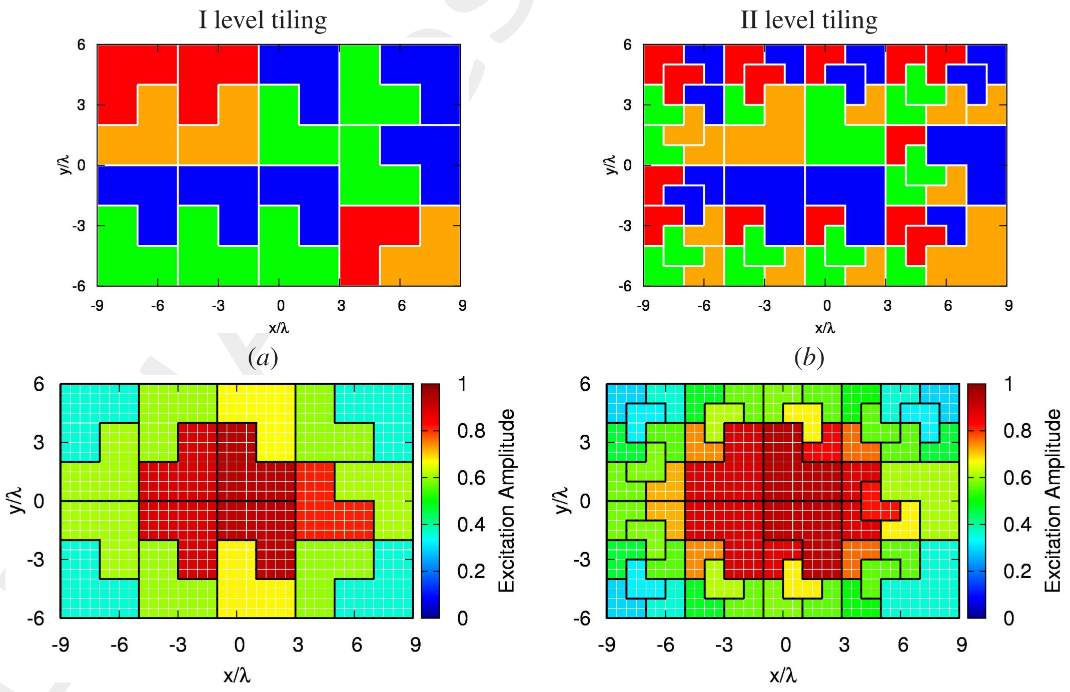

(c) (d)

Figure 21: Numerical Assessment ($M = 24$, $N = 36$, $d = 0.5\lambda$, (θ_0,ϕ_0)=(0.0, 0.0) [deg]; $\sigma_1 = 6$ and $\sigma_2 = 48$ for $\gamma_1 = 48$ and $\gamma_2 = 12$) - Plots of (a) optimal solution clustering only with I level tiles and of the (b) same solution clustering with twelve clusters tiled with II level subclusters, with the respective (c) clustered excitations value for the I level solution and (d) the clustered excitations for the II level solution.

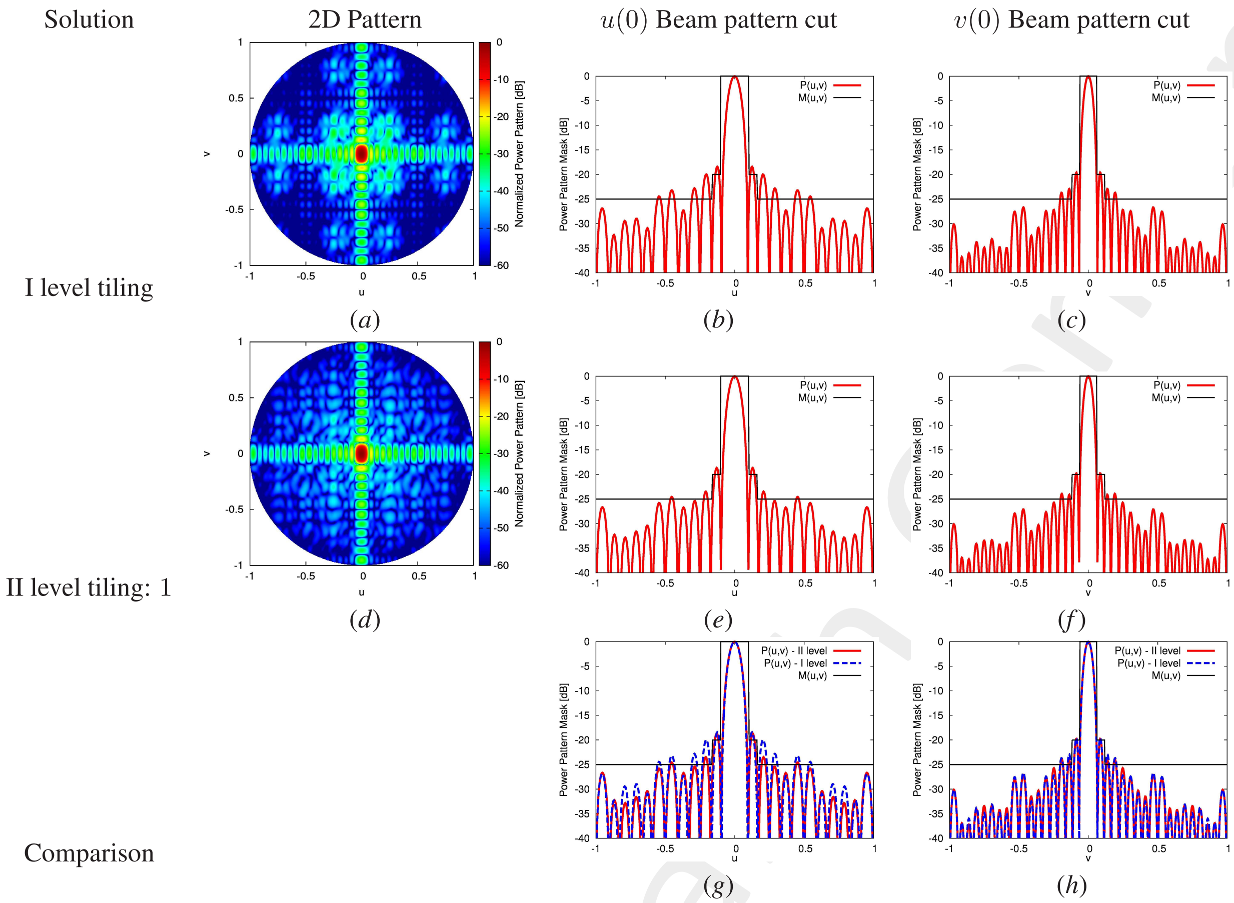

Figure 22: Numerical Assessment ($M = 24,\ N = 36$, $d = 0.5\lambda$, (θ_0,ϕ_0)=(0.0, 0.0) [deg]; $\sigma_1 = 6$ and $\sigma_2 = 48$ for $\gamma_1 = 48$ and $\gamma_2 = 12$) - Plots of normalized power pattern radiated in the whole angular range ($-1 \leq u \leq 1,\ -1 \leq v \leq 1$) for ($a$) the I level clustering, (d) II level clustering and, along the $\phi = 0$ [deg] plane for I level (b), II level (e) and the comparison between both (g) cases, and along the $\phi = 90$ [deg] plane for I level (c), II level (f) and comparison between both (h) solution

Solution	SLL $[dB]$	Max. Directivity $[dBi]$	Mask Matching	HPBW (AZ) $[deg]$	HPBW (EL) $[deg]$
I level	-18.408	33.881	0.292×10^{-4}	3.14	4.57
II level	-18.657	33.837	0.529×10^{-5}	3.15	4.69
Fully populated	-19.958	33.828	0.393×10^{-9}	3.17	4.77

Table VII: Numerical Assessment ($M = 24,\ N = 36$, $d = 0.5\lambda$, (θ_0,ϕ_0)=(0.0, 0.0) [deg] - Pattern features

Parameters - II level clustering on all tiles:

- Number of elements: 24×36 elements array
- Number of rows: $M = 24$ Number of columns: $N = 36$
- Number of clusters:$\sigma_2 = 72$
- Clusters elements: $\gamma_2 = 12$
- Samples: $u \to 702$, $v \to 462$
- Elements spacing: $dx = dy = 0.5\lambda$

The cost function only considers the mask matching.

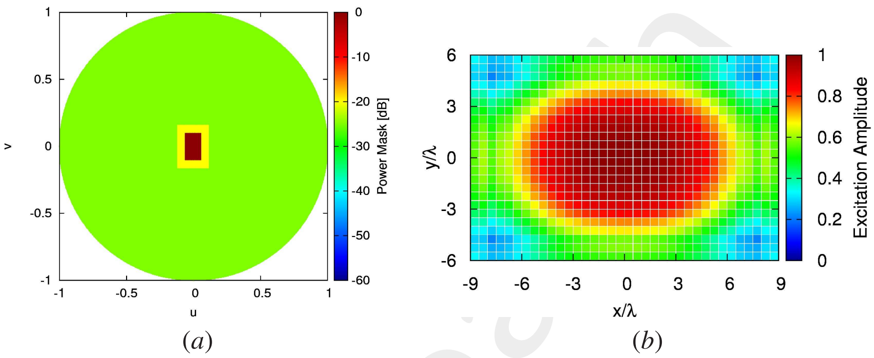

Figure 23: (a) Mask used for the computation of the cost function (b) Reference amplitudes

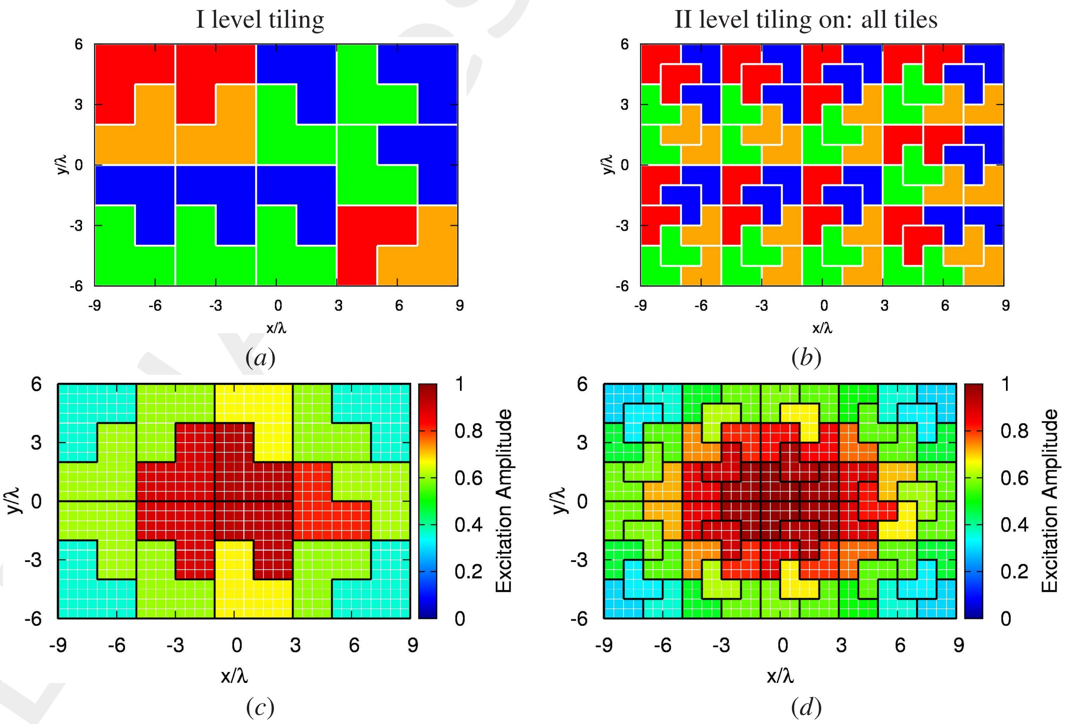

Figure 24: Numerical Assessment ($M = 24,\ N = 36$, $d = 0.5\lambda$, (θ_0,ϕ_0)=(0.0, 0.0) [deg]; $\sigma_2 = 72$ $\gamma_2 = 12$) - Plots of (a) optimal solution clustering only with I level tiles and of the (b) same solution clustering for all the tiles tiled with II level subclusters, with the respective (c) clustered excitations value for the I level solution and (d) the clustered excitations for the II level solution.

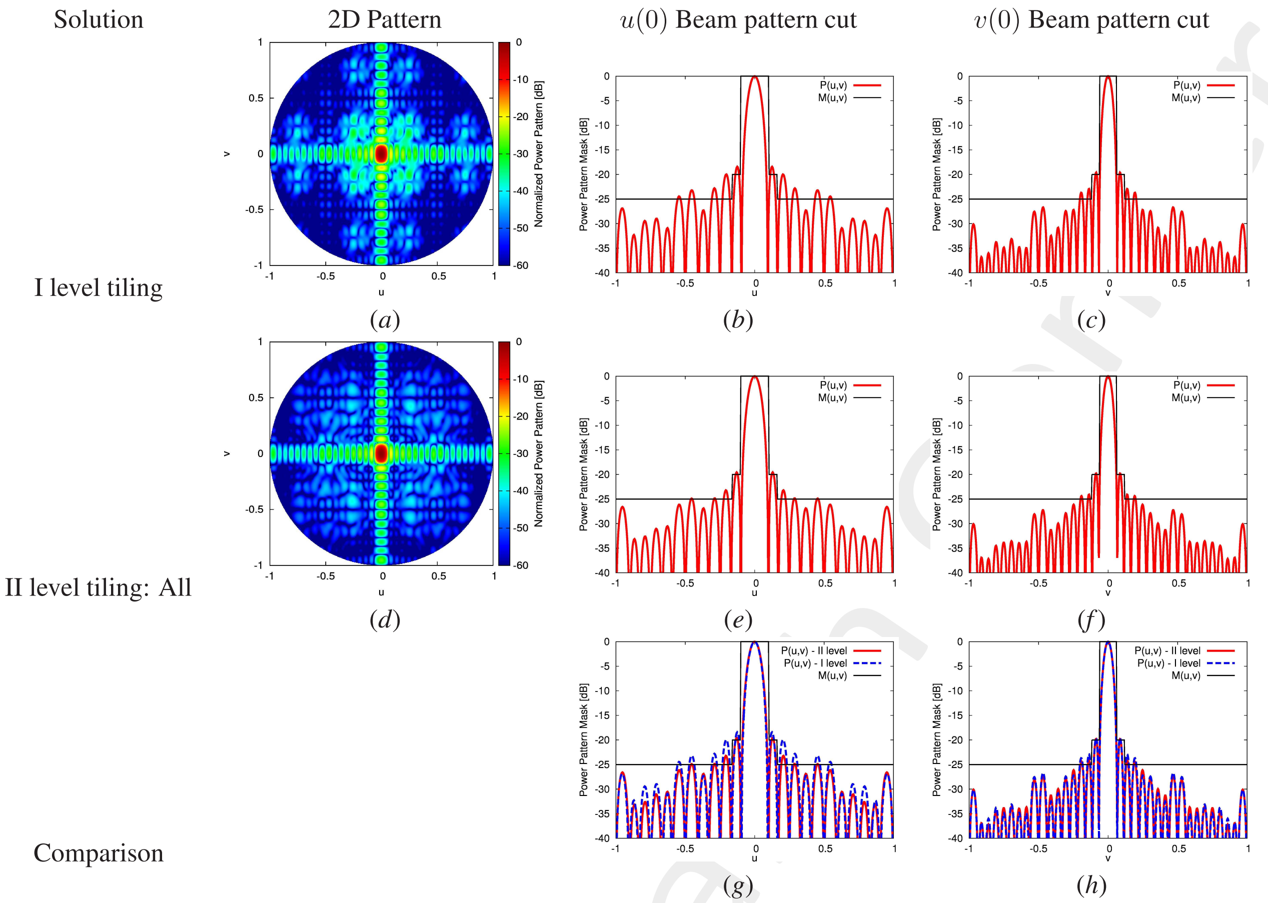

Figure 25: Numerical Assessment ($M = 24,\ N = 36$, $d = 0.5\lambda$, (θ_0,ϕ_0)=(0.0, 0.0) [deg]; $\sigma_2 = 72$ for $\gamma_2 = 12$) - Plots of normalized power pattern radiated in the whole angular range ($-1 \leq u \leq 1,\ -1 \leq v \leq 1$) for ($a$) the I level clustering, (d) II level clustering and, along the $\phi = 0$ [deg] plane for I level (b), II level (e) and the comparison between both (g) cases, and along the $\phi = 90$ [deg] plane for I level (c), II level (f) and comparison between both (h) solution

Solution	SLL $[dB]$	Max. Directivity $[dBi]$	Mask Matching	HPBW (AZ) $[deg]$	HPBW (EL) $[deg]$
I level	-18.408	33.881	0.292×10^{-4}	3.14	4.57
II level	-19.563	33.825	0.267×10^{-5}	3.16	4.72
Fully populated	-19.958	33.828	0.393×10^{-9}	3.17	4.77

Table VIII: Numerical Assessment ($M = 24,\ N = 36$, $d = 0.5\lambda$, (θ_0,ϕ_0)=(0.0, 0.0) [deg] - Pattern features

Third Level Clustering

If Γ is lower once a second level tile is third level clustered we can keep reclustering, otherwise there are two options/algorithms

1. Change reclustered tile until one that lowers Γ is found
2. Stop when Γ increases (even once)

Using the same priority criteria of Sect. 1.1 (Integral Difference) the priority has been computed each time a new tile has been reclustered from first to second level, to find out if there were third level reclusterings with higher priority than second level.

The results show that no third level reclustering has higher priority than second level ones.

Three experiments have been performed starting from already studied results.

Starting Point: 6 Second Level Tiles Starting from the array clustered with 6 second level clustered tiles, third level clustering has been applied.

Using algorithm 1) the results are shown in the following table:

Iteration	Initial Γ	1 Tile	q_1	2 Tiles	q_2
1	0.998×10^{-5}	0.967×10^{-5}	18	0.977×10^{-5}	24
2				0.977×10^{-5}	16
3				0.973×10^{-5}	29
4				0.965×10^{-5}	8

Table IX: Results for Algorithm 1)

Using algorithm 2) the results are shown in the following table:

Initial Γ	1 Tile	q	2 Tiles	q	4 Tiles	q
0.998×10^{-5}	0.967×10^{-5}	18	0.977×10^{-5}	24	0.973×10^{-5}	29+16

Table X: Results for Algorithm 2)

Starting Point: 12 Second Level Tiles Starting from the array clustered with 12 second level clustered tiles, third level clustering has been applied.

Using algorithm 1) the results are shown in the following table:

Iteration	Initial Γ	1 Tile	q_1	2 Tiles	q_2
1	0.529×10^{-5}	0.506×10^{-5}	18	0.507×10^{-5}	24
2				0.513×10^{-5}	16
3				0.511×10^{-5}	29
4				0.508×10^{-5}	8

Table XI: Results for Algorithm 1)

Using algorithm 2) the results are shown in the following table:

Initial Γ	1 Tile	q	2 Tiles	q	4 Tiles	q
0.529×10^{-5}	0.506×10^{-5}	18	0.507×10^{-5}	24	0.537×10^{-5}	29+16

Table XII: Results for Algorithm 2)

L-Tromino, *Second Level Clustering* - Amplitude Difference Priority

For the second iteration it is possible to choose which tile of the "First Level" divide: the chosen criteria is to increase the number of tiles where the difference between the amplitudes in the same cluster is larger: following this method the results are the following:

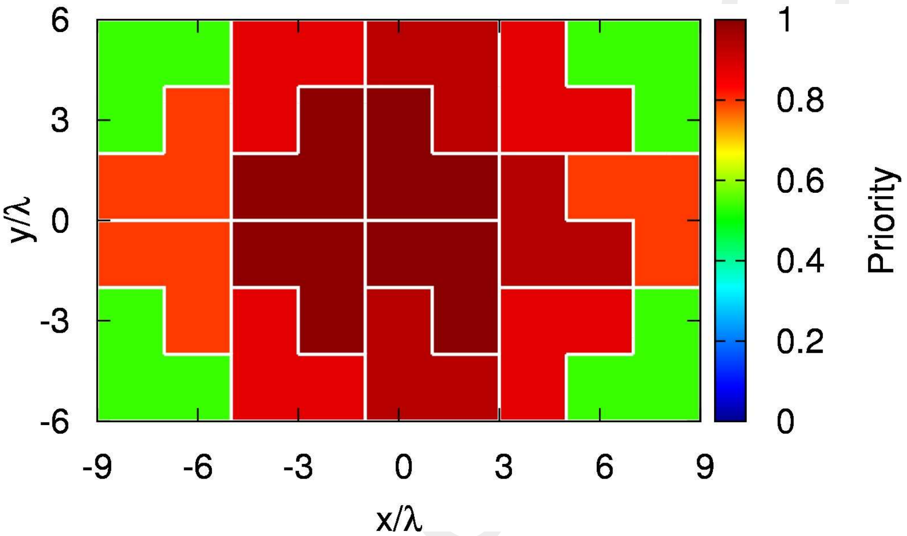

Figure 26: Difference between amplitudes in the same cluster

1.1.1 Parameters - II level clustering on the two highest priority tiles:

- Number of elements: 24×36 elements array, grouped in 24 clusters: two clusters of 12 elements and 16 of 48 elements
- Number of rows: 24
- Number of columns: 36
- Samples: $u \rightarrow 702$, $v \rightarrow 462$
- Elements spacing: $dx = dy = 0.5\lambda$

The cost function only considers the mask matching.

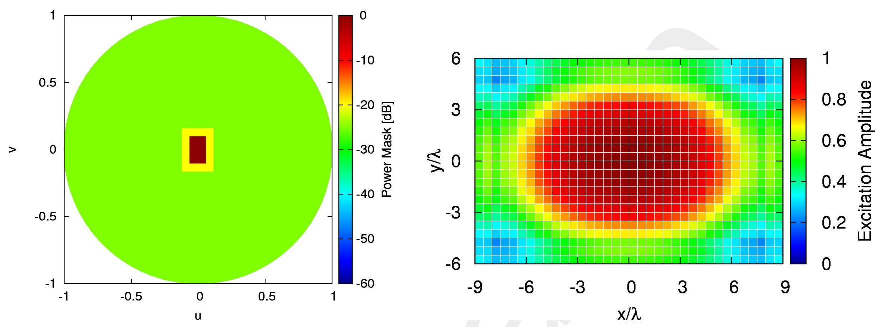

(a) (b)

Figure 27: (a) Mask used for the computation of the cost function (b) Reference amplitudes

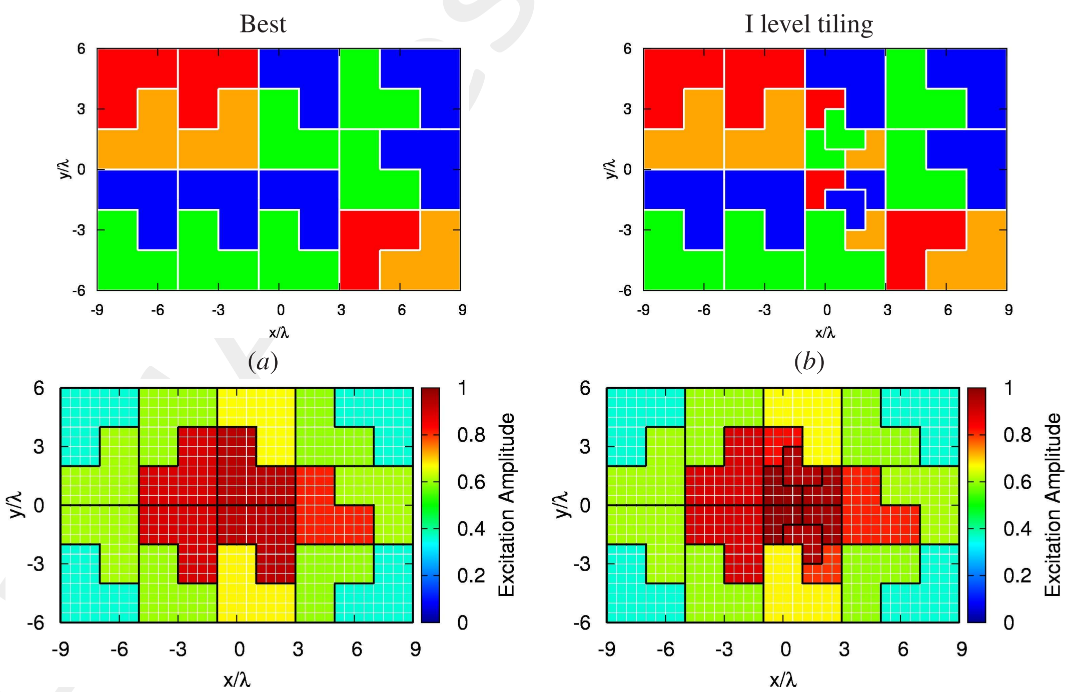

(a) (b) (c) (d)

Figure 28: Numerical Assessment ($M = 24$, $N = 36$, $d = 0.5\lambda$, (θ_0, ϕ_0)=(0.0, 0.0) [deg]; $Q_I = 16$ and $Q_{II} = 8$ for $I = 48$ and $II = 12$) - Plots of (a) optimal solution clustering only with I level tiles and of the (b) same solution clustering with the two highest priority tiles tiled with II level subclusters, with the respective (c) clustered excitations value for the I level solution and (d) the clustered excitations for the II level solution.

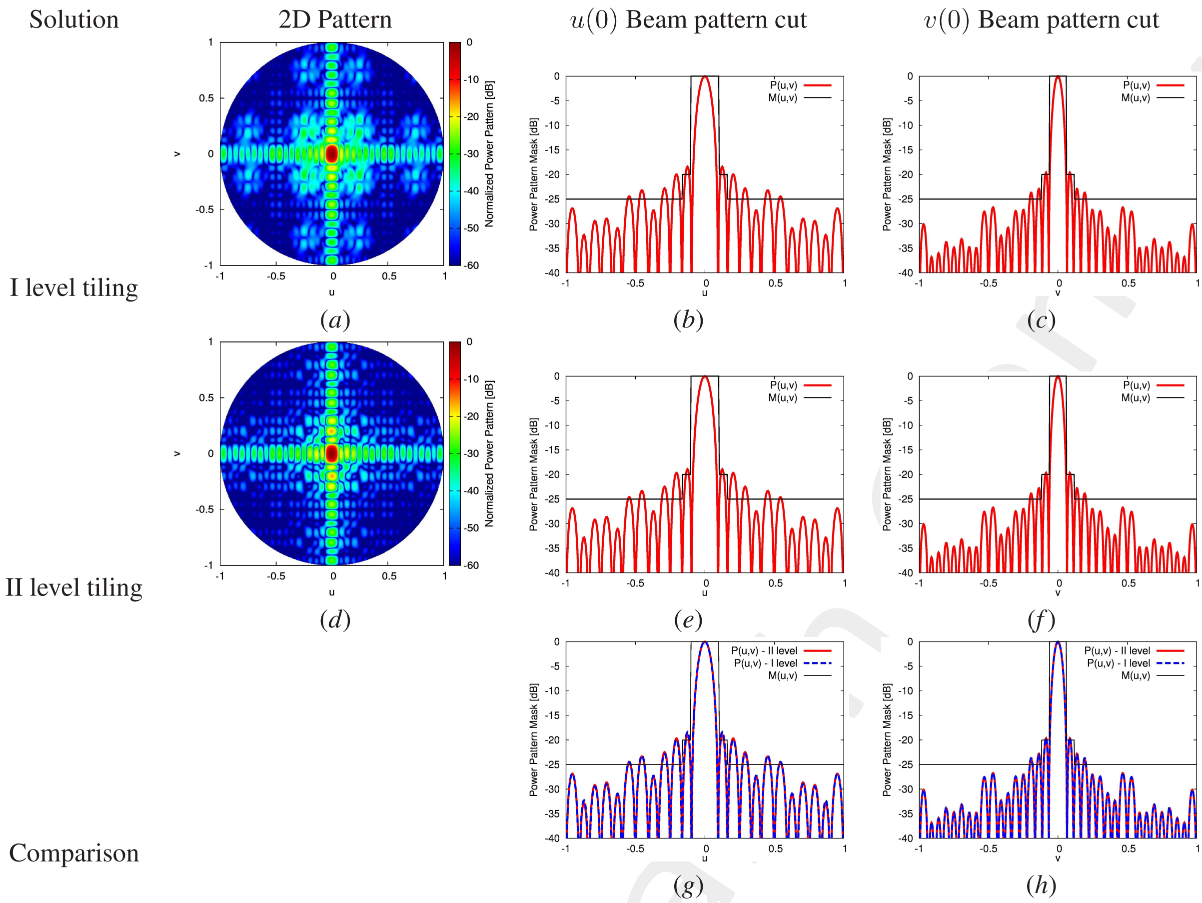

Figure 29: Numerical Assessment ($M = 24,\ N = 36$, $d = 0.5\lambda$, (θ_0,ϕ_0)=(0.0, 0.0) [deg]; $Q_I = 16$ and $Q_{II} = 8$ for $I = 48$ and $II = 24$) - Plots of normalized power pattern radiated in the whole angular range ($-1 \leq u \leq 1,\ -1 \leq v \leq 1$) for (*a*) the I level clustering, (*d*) II level clustering and, along the $\phi = 0$ [deg] plane for I level (*b*), II level (*e*) and the comparison between both (*g*) cases, and along the $\phi = 90$ [deg] plane for I level (*c*), II level (*f*) and comparison between both (*h*) solution

Solution	SLL $[dB]$	Max. Directivity $[dBi]$	Mask Matching	HPBW (AZ) $[deg]$	HPBW (EL) $[deg]$
I level	-18.408	33.881	0.292×10^{-4}	3.14	4.57
II level	-18.911	33.876	0.307×10^{-4}	3.14	4.58
Fully populated	-19.958	33.828	0.393×10^{-9}	3.17	4.77

Table XIII: Numerical Assessment ($M = 24,\ N = 36$, $d = 0.5\lambda$, (θ_0,ϕ_0)=(0.0, 0.0) [deg] - Pattern features

1.1.2 Parameters - II level clustering on all tiles:

- Number of elements: 24×36 elements array, grouped in 72 clusters of 12 elements
- Number of rows: 24
- Number of columns: 36
- Samples: $u \rightarrow 702$, $v \rightarrow 462$
- Elements spacing: $dx = dy = 0.5\lambda$

The cost function only considers the mask matching.

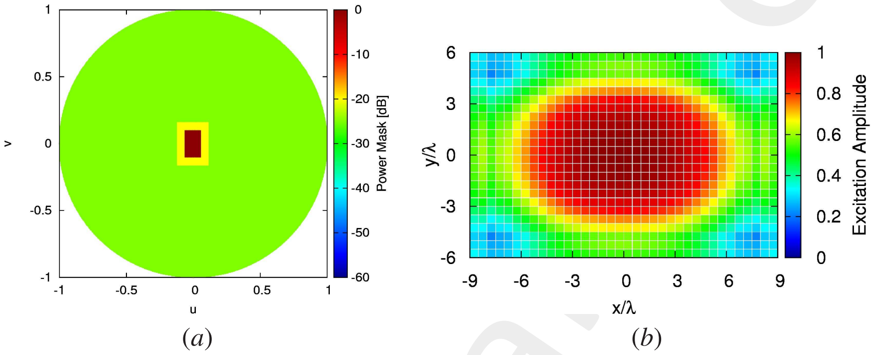

Figure 30: (a) Mask used for the computation of the cost function (b) Reference amplitudes

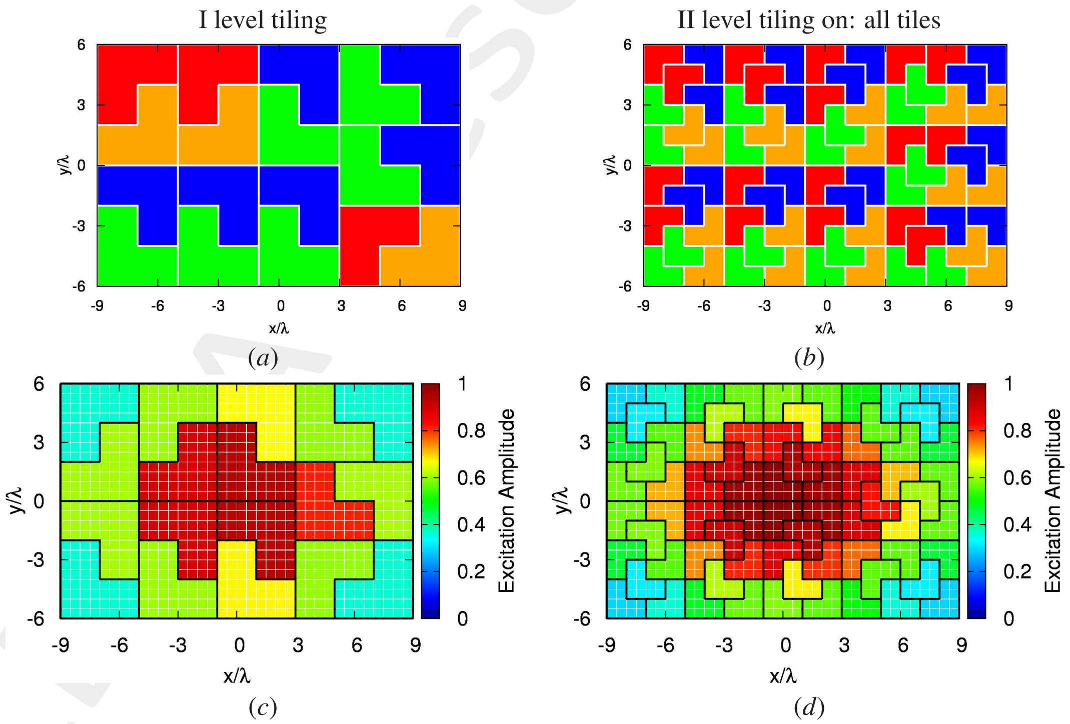

Figure 31: Numerical Assessment ($M = 24,\ N = 36$, $d = 0.5\lambda$, (θ_0,ϕ_0)=(0.0, 0.0) [deg]; $Q_{II} = 72\ II = 12$) - Plots of (a) optimal solution clustering only with I level tiles and of the (b) same solution clustering for all the tiles tiled with II level subclusters, with the respective (c) clustered excitations value for the I level solution and (d) the clustered excitations for the II level solution.

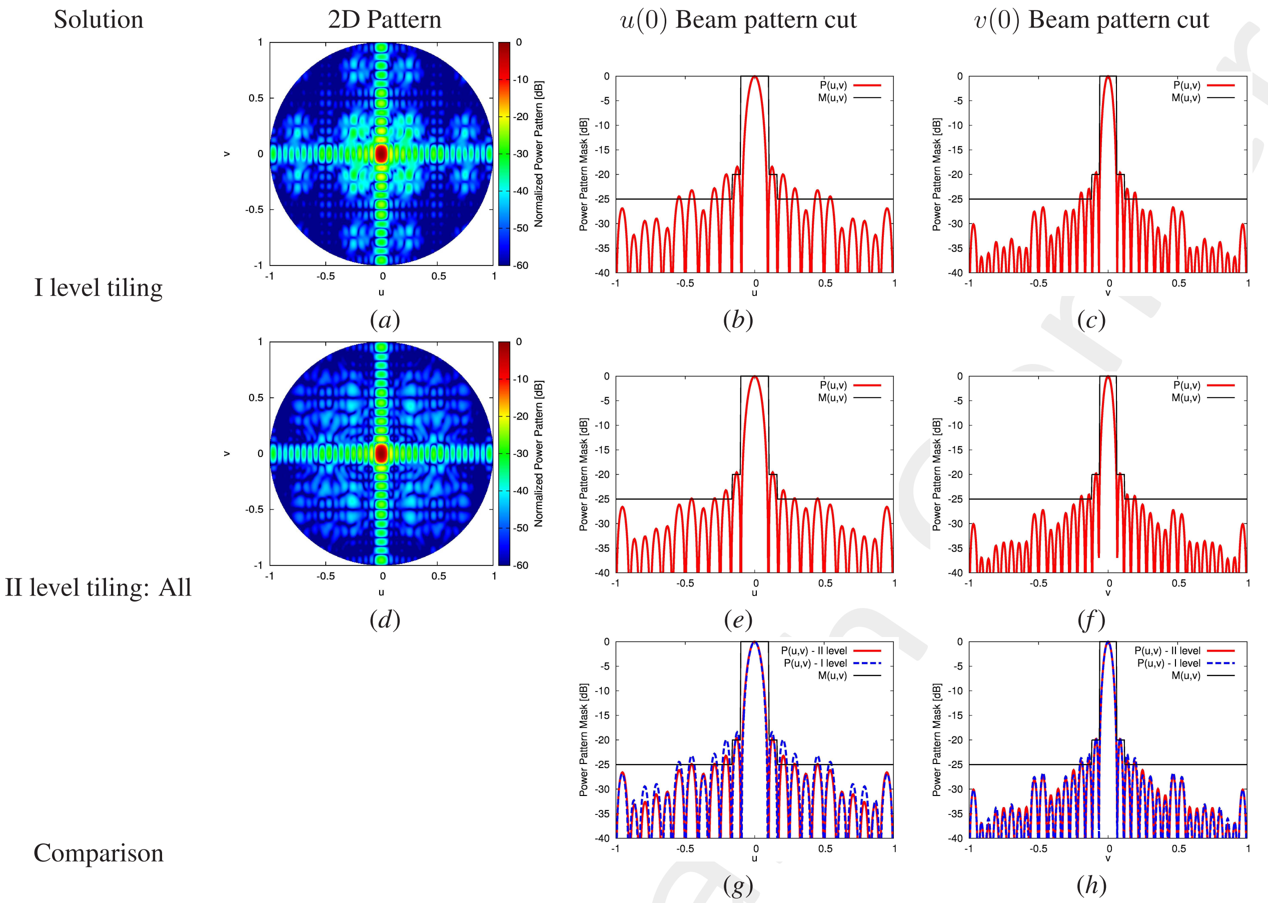

Figure 32: Numerical Assessment ($M = 24,\ N = 36$, $d = 0.5\lambda$, (θ_0,ϕ_0)=(0.0, 0.0) [deg]; $Q_{II} = 72$ for $II = 24$) - Plots of normalized power pattern radiated in the whole angular range ($-1 \leq u \leq 1,\ -1 \leq v \leq 1$) for ($a$) the I level clustering, (d) II level clustering and, along the $\phi = 0$ [deg] plane for I level (b), II level (e) and the comparison between both (g) cases, and along the $\phi = 90$ [deg] plane for I level (c), II level (f) and comparison between both (h) solution

Solution	SLL $[dB]$	Max. Directivity $[dBi]$	Mask Matching	HPBW (AZ) $[deg]$	HPBW (EL) $[deg]$
I level	-18.408	33.881	0.292×10^{-4}	3.14	4.57
II level	-19.563	33.825	0.267×10^{-5}	3.16	4.72
Fully populated	-19.958	33.828	0.393×10^{-9}	3.17	4.77

Table XIV: Numerical Assessment ($M = 24,\ N = 36$, $d = 0.5\lambda$, (θ_0,ϕ_0)=(0.0, 0.0) [deg] - Pattern features

1.1.3 Parameters - II level clustering on a low priority tile:

- Number of elements: 24×36 elements array, grouped in 21 clusters: one cluster of 12 elements and 17 of 48 elements
- Number of rows: 24
- Number of columns: 36
- Samples: $u \rightarrow 702$, $v \rightarrow 462$
- Elements spacing: $dx = dy = 0.5\lambda$

The cost function only considers the mask matching.

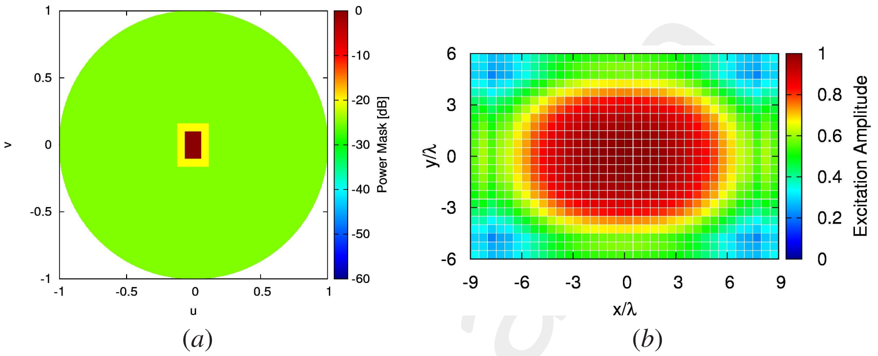

Figure 33: (a) Mask used for the computation of the cost function (b) Reference amplitudes

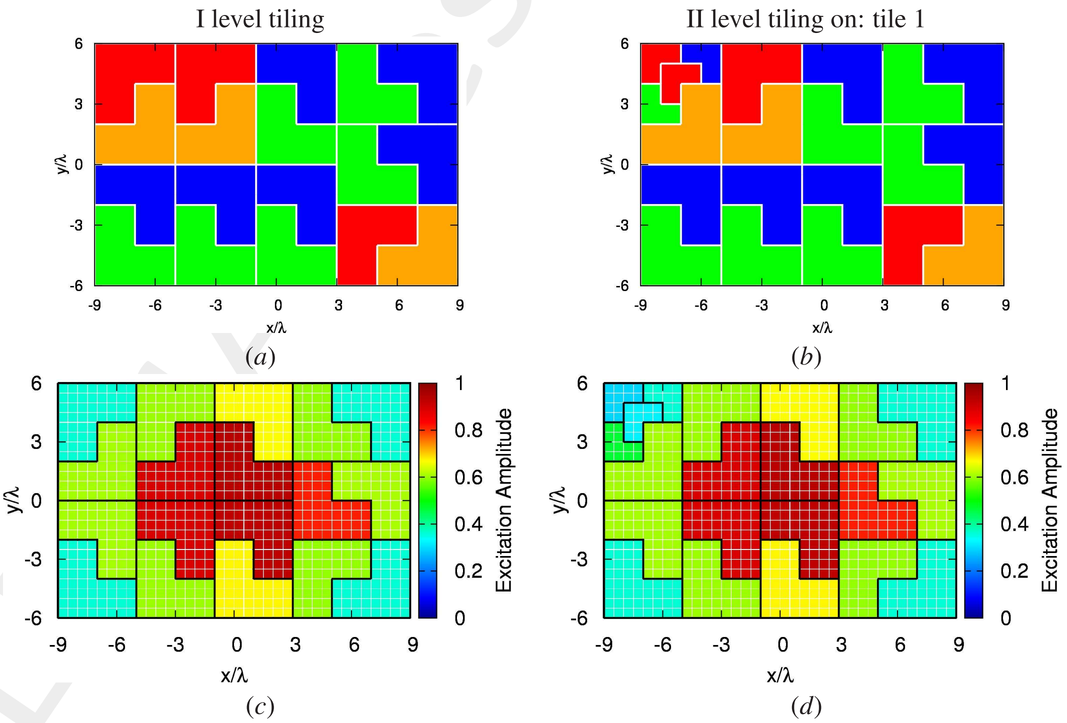

Figure 34: Numerical Assessment ($M = 24,\ N = 36$, $d = 0.5\lambda$, (θ_0,ϕ_0)=(0.0, 0.0) [deg]; $Q_I = 17$ and $Q_{II} = 4$ for $II = 12$) - Plots of (a) optimal solution clustering only with I level tiles and of the (b) same solution clustering with one single low priority tile tiled with II level subclusters, with the respective (c) clustered excitations value for the I level solution and (d) the clustered excitations for the II level solution.

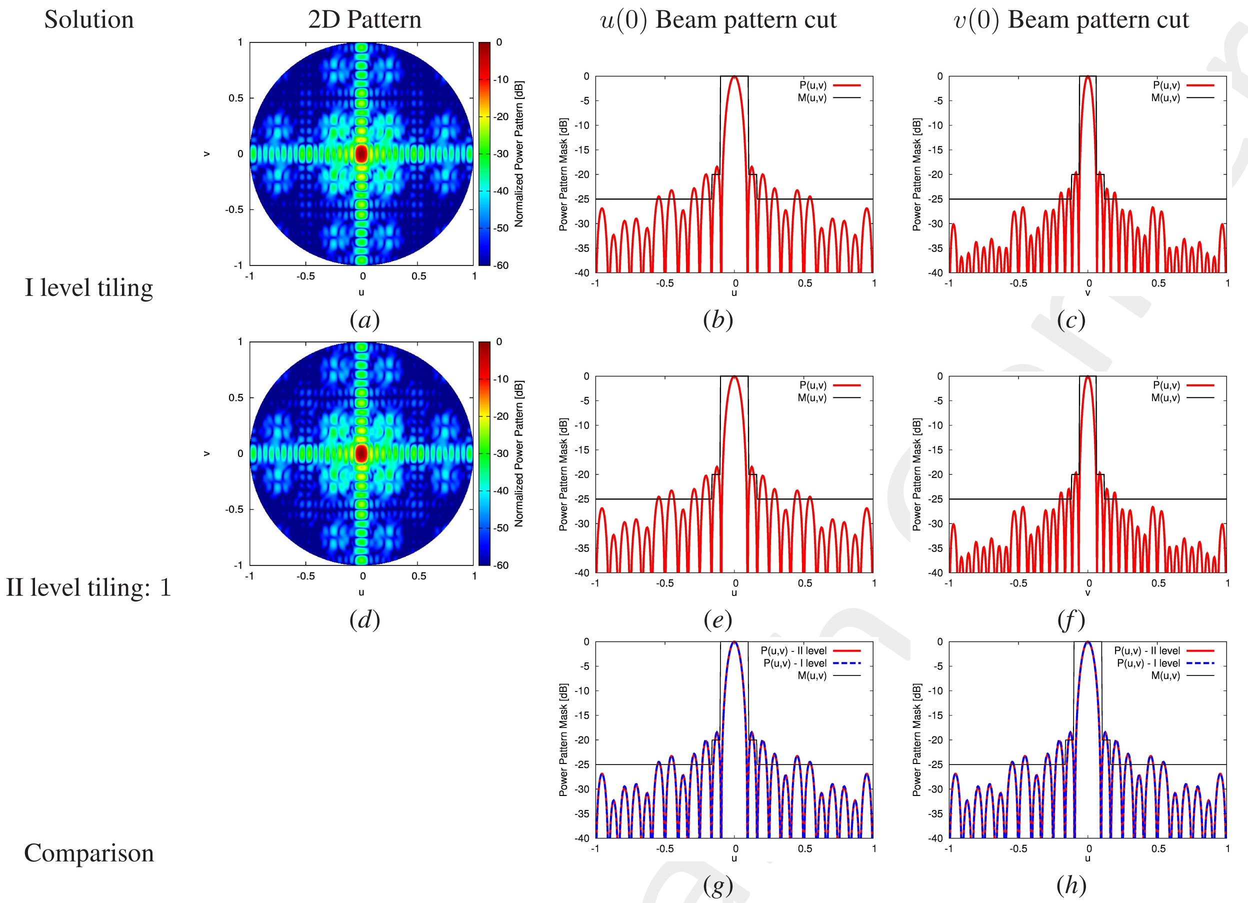

Figure 35: Numerical Assessment ($M = 24,\ N = 36$, $d = 0.5\lambda$, (θ_0,ϕ_0)=(0.0, 0.0) [deg]; $Q_I = 17$ and $Q_{II} = 4$ for $I = 48$ and $II = 24$) - Plots of normalized power pattern radiated in the whole angular range ($-1 \leq u \leq 1,\ -1 \leq v \leq 1$) for (*a*) the I level clustering, (*d*) II level clustering and, along the $\phi = 0$ [deg] plane for I level (*b*), II level (*e*) and the comparison between both (*g*) cases, and along the $\phi = 90$ [deg] plane for I level (*c*), II level (*f*) and comparison between both (*h*) solution

Solution	SLL $[dB]$	Max. Directivity $[dBi]$	Mask Matching	HPBW (AZ) $[deg]$	HPBW (EL) $[deg]$
I level	-18.408	33.881	0.292×10^{-4}	3.14	4.57
II level	-18.400	33.878	0.272×10^{-4}	3.14	4.58
Fully populated	-19.958	33.828	0.393×10^{-9}	3.17	4.77

Table XV: Numerical Assessment ($M = 24,\ N = 36$, $d = 0.5\lambda$, (θ_0,ϕ_0)=(0.0, 0.0) [deg] - Pattern features

More information on the topics of this document can be found in the following list of references.

References

[1] N. Anselmi, L. Tosi, P. Rocca, G. Toso, and A. Massa, “A self-replicating single-shape tiling technique for the design of highly modular planar phased arrays - The case of L-shaped rep-tiles,” *IEEE Trans. Antennas Propag.* , vol. 71, no. 4, pp. 3335-3348, Apr. 2023.

[2] A. Benoni, P. Rocca, N. Anselmi, and A. Massa, “Hilbert-ordering based clustering of complex-excitations linear arrays,” *IEEE Trans. Antennas Propag.* , vol. 70, no. 8, pp. 6751-6762, Aug. 2022.

[3] P. Rocca, L. Poli, N. Anselmi, and A. Massa, “Nested optimization for the synthesis of asymmetric shaped beam patterns in sub-arrayed linear antenna arrays,” *IEEE Trans. Antennas Propag.* , vol. 70, no. 5, pp. 3385 - 3397, May 2022.

[4] P. Rocca, L. Poli, A. Polo, and A. Massa, “Optimal excitation matching strategy for sub-arrayed phased linear arrays generating arbitrary shaped beams,” *IEEE Trans. Antennas Propag.*, vol. 68, no. 6, pp. 4638-4647, Jun. 2020.

[5] G. Oliveri, G. Gottardi and A. Massa, “A new meta-paradigm for the synthesis of antenna arrays for future wireless communications,” *IEEE Trans. Antennas Propag.*, vol. 67, no. 6, pp. 3774-3788, Jun. 2019.

[6] P. Rocca, M. H. Hannan, L. Poli, N. Anselmi, and A. Massa, “Optimal phase-matching strategy for beam scanning of sub-arrayed phased arrays,” *IEEE Trans. Antennas and Propag.*, vol. 67, no. 2, pp. 951-959, Feb. 2019.

[7] N. Anselmi, P. Rocca, M. Salucci, and A. Massa, “Contiguous phase-clustering in multibeam-on-receive scanning arrays,” *IEEE Trans. Antennas Propag.*, vol. 66, no. 11, pp. 5879-5891, Nov. 2018.

[8] L. Poli, G. Oliveri, P. Rocca, M. Salucci, and A. Massa, “Long-Distance WPT Unconventional Arrays Synthesis,” *J. Electromagn. Waves Appl.* J, vol. 31, no. 14, pp. 1399-1420, Jul. 2017.

[9] G. Gottardi, L. Poli, P. Rocca, A. Montanari, A. Aprile, and A. Massa, “Optimal Monopulse Beamforming for Side-Looking Airborne Radars,” *IEEE Antennas Wireless Propag.* Lett., vol. 16, pp. 1221-1224, 2017.

[10] G. Oliveri, M. Salucci, and A. Massa, “Synthesis of modular contiguously clustered linear arrays through a sparseness-regularized solver,” *IEEE Trans. Antennas Propag.*, vol. 64, no. 10, pp. 4277-4287, Oct. 2016.

[11] P. Rocca, G. Oliveri, R. J. Mailloux, and A. Massa, “Unconventional phased array architectures and design Methodologies - A review,” *Proc. IEEE*, Invited Paper, vol. 104, no. 3, pp. 544-560, March 2016.

[12] P. Rocca, M. D’Urso, and L. Poli,"Advanced strategy for large antenna array design with subarray-only amplitude and phase control,” *IEEE Antennas and Wireless Propag. Lett.*, vol. 13, pp. 91-94, 2014.

[13] L. Manica, P. Rocca, G. Oliveri, and A. Massa, “Synthesis of multi-beam sub-arrayed antennas through an excitation matching strategy,” *IEEE Trans. Antennas Propag.*, vol. 59, no. 2, pp. 482-492, Feb. 2011.

[14] G. Oliveri, "Multi-beam antenna arrays with common sub-array layouts," *IEEE Antennas Wireless Propag. Lett.*, vol. 9, pp. 1190-1193, 2010.

[15] P. Rocca, R. Haupt, and A. Massa, "Sidelobe reduction through element phase control in sub-arrayed array antennas," *IEEE Antennas Wireless Propag. Lett.*, vol. 8, pp. 437-440, 2009.

[16] P. Rocca, L. Manica, R. Azaro, and A. Massa, "A hybrid approach for the synthesis of sub-arrayed monopulse linear arrays," *IEEE Trans. Antennas Propag.* , vol. 57, no. 1, pp. 280-283, Jan. 2009.

[17] L. Manica, P. Rocca, M. Benedetti, and A. Massa, "A fast graph-searching algorithm enabling the efficient synthesis of sub-arrayed planar monopulse antennas," *IEEE Trans. Antennas Propag.*, vol. 57, no. 3, pp. 652-664, Mar. 2009.

[18] P. Rocca, L. Manica, A. Martini, and A. Massa, "Compromise sum-difference optimization through the iterative contiguous partition method," *IET Microwaves, Antennas & Propagation*, vol. 3, no. 2, pp. 348-361, 2009.

[19] L. Manica, P. Rocca, and A. Massa, "An excitation matching procedure for sub-arrayed monopulse arrays with maximum directivity," *IET Radar, Sonar & Navigation*, vol. 3, no. 1, pp. 42-48, Feb. 2009.

[20] L. Manica, P. Rocca, and A. Massa, "Design of subarrayed linear and planar array antennas with SLL control based on an excitation matching approach," *IEEE Trans. Antennas Propag.*, vol. 57, no. 6, pp. 1684-1691, Jun. 2009.

[21] L. Manica, P. Rocca, A. Martini, and A. Massa, "An innovative approach based on a tree-searching algorithm for the optimal matching of independently optimum sum and difference excitations," *IEEE Trans. Antennas Propag.*, vol. 56, no. 1, pp. 58-66, Jan. 2008.

[22] P. Rocca, L. Manica, and A. Massa, "An effective excitation matching method for the synthesis of optimal compromises between sum and difference patterns in planar arrays," *Progress in Electromagnetic Research B*, vol. 3, pp. 115-130, 2008.

[23] P. Rocca, L. Manica, and A. Massa, "Directivity optimization in planar sub-arrayed monopulse antenna," *Progress in Electromagnetic Research L*, vol. 4, pp. 1-7, 2008.

[24] P. Rocca, L. Manica, M. Pastorino, and A. Massa, "Boresight slope optimization of sub-arrayed linear arrays through the contiguous partition method," *IEEE Antennas Wireless Propag. Lett.*, vol. 8, pp. 253-257, 2008.

[25] P. Rocca, L. Manica, and A. Massa, "Synthesis of monopulse antennas through the iterative contiguous partition method," *Electronics Letters*, vol. 43, no. 16, pp. 854-856, Aug. 2007.

[26] P. Rocca, L. Manica, A. Martini, and A. Massa, "Synthesis of large monopulse linear arrays through a tree-based optimal excitations matching," *IEEE Antennas Wireless Propag. Lett.*, vol. 7, pp. 436-439, 2007.

[27] P. Rocca, N. Anselmi, A. Polo, and A. Massa, "Pareto-optimal domino-tiling of orthogonal polygon phased arrays, " *IEEE Trans. Antennas Propag.*, vol. 70, no. 5, pp. 3329-3342, May 2022.

[28] P. Rocca, N. Anselmi, A. Polo, and A. Massa, "An irregular two-sizes square tiling method for the design of isophoric phased arrays, " *IEEE Trans. Antennas Propag.*, vol. 68, no. 6, pp. 4437-4449, Jun. 2020.

[29] P. Rocca, N. Anselmi, A. Polo, and A. Massa, "Modular design of hexagonal phased arrays through diamond tiles, " IEEE Trans. Antennas Propag., vol.68, no. 5, pp. 3598-3612, May 2020.

[30] N. Anselmi, L. Poli, P. Rocca, and A. Massa, "Design of simplified array layouts for preliminary experimental testing and validation of large AESAs, " *IEEE Trans. Antennas Propag.*, vol. 66, no. 12, pp. 6906-6920, Dec. 2018.

[31] G. Oliveri, G. Gottardi, F. Robol, A. Polo, L. Poli, M. Salucci, M. Chuan, C. Massagrande, P. Vinetti, M. Mattivi, R. Lombardi, and A. Massa, "Co-design of unconventional array architectures and antenna elements for 5G base station, " *IEEE Trans. Antennas Propag.*, vol. 65, no. 12, pp. 6752-6767, Dec. 2017.

[32] N. Anselmi, P. Rocca, M. Salucci, and A. Massa, "Irregular phased array tiling by means of analytic schemata-driven optimization, " *IEEE Trans. Antennas Propag.*, vol. 65, no. 9, pp. 4495-4510, September 2017.

[33] N. Anselmi, P. Rocca, M. Salucci, and A. Massa, "Optimization of excitation tolerances for robust beamforming in linear arrays," *IET Microwaves*, Antennas & Propagation, vol. 10, no. 2, pp. 208-214, 2016.

[34] P. Rocca, R. J. Mailloux, and G. Toso, "GA-Based optimization of irregular sub-array layouts for wideband phased arrays desig, " *IEEE Antennas and Wireless Propag. Lett.*, vol. 14, pp. 131-134, 2015.

[35] P. Rocca, M. Donelli, G. Oliveri, F. Viani, and A. Massa, "Reconfigurable sum-difference pattern by means of parasitic elements for forward-looking monopulse radar, " *IET Radar, Sonar & Navigation*, vol 7, no. 7, pp. 747-754, 2013.

[36] P. Rocca, L. Manica, and A. Massa, "Ant colony based hybrid approach for optimal compromise sum-difference patterns synthesis, " *Microwave Opt. Technol. Lett.*, vol. 52, no. 1, pp. 128-132, Jan. 2010.

[37] P. Rocca, L. Manica, and A. Massa, "An improved excitation matching method based on an ant colony optimization for suboptimal-free clustering in sum-difference compromise synthesis, " *IEEE Trans. Antennas Propag.*, vol. 57, no. 8, pp. 2297-2306, Aug. 2009.

[38] P. Rocca, L. Manica, and A. Massa, "Hybrid approach for sub-arrayed monopulse antenna synthesis, " *Electronics Letters*, vol. 44, no. 2, pp. 75-76, Jan. 2008.

[39] P. Rocca, L. Manica, F. Stringari, and A. Massa, "Ant colony optimization for tree-searching based synthesis of monopulse array antenna, " *Electronics Letters*, vol. 44, no. 13, pp. 783-785, Jun. 19, 2008.